Restudy of *Liaoningotitan sinensis* Zhou *et al.*, 2018 (#104464)

First submission

Guidance from your Editor

Please submit by **23 Sep 2024** for the benefit of the authors (and your token reward) .

Structure and Criteria
Please read the 'Structure and Criteria' page for guidance.

Raw data check
Review the raw data.

Image check
Check that figures and images have not been inappropriately manipulated.

If this article is published your review will be made public. You can choose whether to sign your review. If uploading a PDF please remove any identifiable information (if you want to remain anonymous).

Files
Download and review all files from the materials page.

12 Figure file(s)
4 Table file(s)
1 Other file(s)

Structure and Criteria

Structure your review

The review form is divided into 5 sections. Please consider these when composing your review:

1. **BASIC REPORTING**
2. **EXPERIMENTAL DESIGN**
3. **VALIDITY OF THE FINDINGS**
4. General comments
5. Confidential notes to the editor

You can also annotate this PDF and upload it as part of your review

When ready submit online.

Editorial Criteria

Use these criteria points to structure your review. The full detailed editorial criteria is on your guidance page.

BASIC REPORTING

- Clear, unambiguous, professional English language used throughout.
- Intro & background to show context. Literature well referenced & relevant.
- Structure conforms to PeerJ standards, discipline norm, or improved for clarity.
- Figures are relevant, high quality, well labelled & described.
- Raw data supplied (see PeerJ policy).

EXPERIMENTAL DESIGN

- Original primary research within Scope of the journal.
- Research question well defined, relevant & meaningful. It is stated how the research fills an identified knowledge gap.
- Rigorous investigation performed to a high technical & ethical standard.
- Methods described with sufficient detail & information to replicate.

VALIDITY OF THE FINDINGS

- **Impact and novelty is not assessed.** Meaningful replication encouraged where rationale & benefit to literature is clearly stated.
- All underlying data have been provided; they are robust, statistically sound, & controlled.
- Conclusions are well stated, linked to original research question & limited to supporting results.

Standout reviewing tips

The best reviewers use these techniques

Tip	*Example*
Support criticisms with evidence from the text or from other sources	*Smith et al (J of Methodology, 2005, V3, pp 123) have shown that the analysis you use in Lines 241-250 is not the most appropriate for this situation. Please explain why you used this method.*
Give specific suggestions on how to improve the manuscript	*Your introduction needs more detail. I suggest that you improve the description at lines 57- 86 to provide more justification for your study (specifically, you should expand upon the knowledge gap being filled).*
Comment on language and grammar issues	*The English language should be improved to ensure that an international audience can clearly understand your text. Some examples where the language could be improved include lines 23, 77, 121, 128 – the current phrasing makes comprehension difficult. I suggest you have a colleague who is proficient in English and familiar with the subject matter review your manuscript, or contact a professional editing service.*
Organize by importance of the issues, and number your points	*1. Your most important issue* *2. The next most important item* *3. …* *4. The least important points*
Please provide constructive criticism, and avoid personal opinions	*I thank you for providing the raw data, however your supplemental files need more descriptive metadata identifiers to be useful to future readers. Although your results are compelling, the data analysis should be improved in the following ways: AA, BB, CC*
Comment on strengths (as well as weaknesses) of the manuscript	*I commend the authors for their extensive data set, compiled over many years of detailed fieldwork. In addition, the manuscript is clearly written in professional, unambiguous language. If there is a weakness, it is in the statistical analysis (as I have noted above) which should be improved upon before Acceptance.*

Restudy of *Liaoningotitan sinensis* Zhou *et al.*, 2018

Bingqing Shan Corresp. [1]

[1] Department of Paleontology college, Shenyang Normal University, Shenyang, Liaoning Province, China

Corresponding Author: Bingqing Shan
Email address: 1790124692@qq.com

Liaoningotitan sinensis Zhou et al., 2018, is one of three Sauropod species that has been found in the Jehol Biota. Liaoningotitan sinensis is from the Lower Cretaceous Yixian Formation in Liaoning, China. The discovery of Liaoningotitan sinensis was an important breakthrough for researching the diversity of giant herbivorous animals in the Jehol Biota, but research and analysis on Liaoningotitan sinensis are not yet complete. This study re-examines Liaoningotitan sinensis using comprehensive and systematic phylogenetic analysis. First, the skull, vertebrae, pelvic girdle, and appendicular skeleton of the Liaoningotitan sinensis holotype were carefully reexamined, leading to the discovery of the mosaic evolution occurring in the skull and the identification of two new identifying characteristics of Liaoningotitan sinensis: the muscle scar located on the anterior surface of the proximal end of the humerus is flat; the anterior surface of the ulnar condyle is divided by a ridge. Second, a reconstruction of the Liaoningotitan sinensis skull was attempted using the characteristics of the Liaoningotitan sinensis holotype and other well-preserved sauropod dinosaurs. Next, Xinjiangtitan shanshanensis was used to reconstruct the Liaoningotitan sinensis holotype body type, with the results indicating it was approximately 13 m in length. Then, TNT software was used to conduct an analysis of the phylogenetic position of Liaoningotitan sinensis, with the results indicating that the Liaoningotitan sinensis can be classified into Euhelopodidae. Finally, an autapomorphic analysis was conducted, with the results indicating that the ulna to humerus length ratio and the tibia to femur length ratio are both autapomorphic characteristics in Liaoningotitan sinensis, but the skull height to skull length ratio is not.

Restudy of *Liaoningotitan sinensis* *Zhou et al., 2018*

Shan Bingqing

Paleontological Museum of Liaoning, Shenyang Normal University, Shenyang 110034, China

Abstract *Liaoningotitan sinensis* Zhou *et al.,* 2018, is one of three Sauropod species that has been found in the Jehol Biota. *Liaoningotitan sinensis* is from the Lower Cretaceous Yixian Formation in Liaoning, China. The discovery of *Liaoningotitan sinensis* was an important breakthrough for researching the diversity of giant herbivorous animals in the Jehol Biota, but research and analysis on *Liaoningotitan sinensis* are not yet complete. This study re-examines *Liaoningotitan sinensis* using comprehensive and systematic phylogenetic analysis. First, the skull, vertebrae, pelvic girdle, and appendicular skeleton of the *Liaoningotitan sinensis* holotype were carefully reexamined, leading to the discovery of the mosaic evolution occurring in the skull and the identification of two new identifying characteristics of *Liaoningotitan sinensis*: the muscle scar located on the anterior surface of the proximal end of the humerus is flat; the anterior surface of the ulnar condyle is divided by a ridge. Second, a reconstruction of the *Liaoningotitan sinensis* skull was attempted using the characteristics of the *Liaoningotitan sinensis* holotype and other well-preserved sauropod dinosaurs. Next, *Xinjiangtitan shanshanensis* was used to reconstruct the *Liaoningotitan sinensis* holotype body type, with the results indicating it was approximately 13 m in length. Then, TNT software was used to conduct an analysis of the phylogenetic position of *Liaoningotitan sinensis*, with the results indicating that the *Liaoningotitan sinensis* can be classified into Euhelopodidae. Finally, an autapomorphic analysis was conducted, with the results indicating that the ulna to humerus length ratio and the tibia to femur length ratio are both autapomorphic characteristics in *Liaoningotitan sinensis*, but the skull height to skull length ratio is not.

Subjects Evolutionary Studies, Paleontology

Keys*: Liaoningotitan sinensis*; Osteology; Sauropod dinosaur; Titanosauriformes; Cretaceous; Euhelopodidae

Introduction

Titanosauriformes is a group of widely-distributed sauropod dinosaurs that flourished during the

Cretaceous period. Extensive fossil evidence has revealed they inhabited all continents, with large populations in South America and East Asia. The majority of Titanosauriformes in East Asia have been discovered in China; as of May 2024, 32 Titanosauriformes species have been named in China. The western part of Liaoning province of China was a distribution region in the Jehol Biota during the Early Cretaceous period. Jehol Biota is notable for its feathered non-avian theropod dinosaurs, early avian theropods, pterosaurs, and early mammals. However, as of May 2024, only three Titanosauriformes had been discovered in Jehol Biota: *Dongbeititan dongi* (Wang *et al.,* 2007), *Liaoningotitan sinensis* (Zhou *et al.,* 2018), and *Ruixinia zhangi* (Mo *et al.,* 2022).

Due to the scarcity of complete, preserved sauropod dinosaur specimens, the characteristic identification and phylogenetic analysis of Titanosauriformes are difficult. Fortunately, compared to most other Titanosauriformes, *Liaoningotitan sinensis* is well preserved, particularly its skull, and the type and structure of the skull reveals characteristics of the transitional phase from early-diverging to late-diverging Titanosauriformes. However, no comprehensive research of *Liaoningotitan sinensis* has yet been conducted. Therefore, it is necessary to assess the osteology of the holotype of *Liaoningotitan sinensis*.

The holotype of *Liaoningotitan sinensis* is housed in the Paleontological Museum of Liaoning, Shenyang Normal University in Liaoning Province, China. It was unearthed in the Xiaobeigou village, Shangyuan town, Beipiao city, Chaoyang city of Liaoning Province (Catalogue number: PMOL-AD00112). This holotype includes a preserved skull with mandibula; partial cervical, dorsal, sacral, and caudal vertebrae; appendicular skeletons; and pelvic girdle.

Figure 1. Geographic provenance of *Liaoningotitan sinensis* (Zhou *et al.,* 2018).

Holotype locality of *Liaoningotitan sinensis* (indicated by red point in left map and green sign in right picture) in Liaoning province, China; Left map copyright: Natural geological explorer

1. Yxian Formation basal conglomeration; 2-3. Yixian Formation andesite; 4. Jianshangou bed; 5. Tuchengzi Formation sandstone; 6. Geological fault; 7. Volcano remains; 8. Fossil site (Adapted from Zhang, 2020).

Table 1. Titanosauriformes in China (adapted from Han *et al.,* 2024)

Methods.

Systematic Paleontology

Saurischia Seeley, 1887

Sauropodomorpha Huene, 1932

Sauropoda Marsh, 1878

Titanosauriformes Salgado *et al.,* 1997

Titanosauria Bonaparte and Coria*,* 1993

Somphospondyli Wilson and Sereno, 1998

Liaoningotitan sinensis Zhou *et al.,* 2018

This study re-examines *Liaoningotitan sinensis* using comprehensive and systematic phylogenetic analysis. First, the skull, vertebrae, pelvic girdle, and appendicular skeleton of the *Liaoningotitan sinensis* holotype were carefully reexamined. Second, a reconstruction of the *Liaoningotitan sinensis* skull was attempted using the characteristics of the *Liaoningotitan sinensis* holotype and other well-preserved sauropod dinosaurs*.* Next, *Xinjiangtitan shanshanensis* was used to reconstruct the *Liaoningotitan sinensis* holotype body type. Then, TNT software was used to conduct an analysis of the phylogenetic position of *Liaoningotitan sinensis*, with the results indicating that the *Liaoningotitan sinensis* can be classified within Euhelopodidae. Finally, an autapomorphic analysis was conducted.

Materials

The skull, partial cervical, dorsal, sacral, and caudal vertebrae; appendicular skeletons and pelvic girdle; the medial and posterior sides of all vertebrae; and most appendicular skeletons of the *Liaoningotitan sinensis* holotype are covered by gypsum. Therefore, the observation and research conducted from this individual specimen is limited.

Diagnosis. The premaxilla is wide, and the ventral region of the maxilla bulges upward. The anterior part of the jugal aligns with the anterior margin of the antorbital fossa. The quadrate branch of the pterygoid is shrunken. The maxilla partly constitutes the antorbital foramen. The teeth on the maxilla are arranged in an imbricated pattern, similar to narrow spoons. The cross-section is D-shaped, with small serrations and no labial groove. The dentary is rectangular in dorsal view, with nine teeth. There are fewer teeth on the dentary than on the maxilla, and they are arranged in a sloping pattern with asymmetrical crowns. The cross-section is elliptical, and the groove and ridge on the lingual side are developed. The basal part of the mandibular teeth crown expands laterally to the lingual side. The width of the proximal end of the humerus is approximately 55% of the total length of the humerus. Two new characteristics were identified: the muscle scar located on the anterior surface of the proximal of the humerus is flat; the anterior surface of the ulnar condyle at the distal end of the humerus is divided by a ridge.

Figure 2. Reconstruction of *Liaoningotitan sinensis* (in left lateral view. Preserved elements of the holotype PMOL-AD00112 in green. Adapted from Bernardo *et al.,* 2016)

Description

Skull: Only the left side of the skull of the *Liaoningotitan sinensis* holotype is visible and is approximately 60 cm in length and 30 cm in height, with no developed premaxillary fenestra. The antorbital fenestra is well defined and triangular, similar to that in *Euhelopus zdanskyi* (Poropat & Benjamin, 2013), *Mamenchisaurus youngi* (Ouyang, 2003), and *Omeisaurus maoianus* (Tang *et al.,* 2001). The narial fenestra opens laterally and does not exhibit a conspicuous expansion from anterior to posterior, similar to that of the early-diverging Titanosauriformes such as *Euhelopus zdanskyi,* but differing from that of the late-diverging Titanosauriformes such as *Rapetosaurus krausei* (Rogers & Forster, 2004). The length of the premaxilla constitutes 15% of the skull's overall length. The length of the maxilla is three times the length of the maxillary teeth arrangement. The maxilla is connected with quadratojugal bone, and the posterior region of the maxilla arches towards the dorsal side, similar to that in the late-diverging Titanosauriformes such as *Rapetosaurus krausei*. The lacrimal expands towards the proximal end and the distal end, and the middle region is thin and inclined to the anterior. The palatine is laminar and triradiate bone, with a maxillary branch. The pterygoid is also triradiate, with a fan-shaped anterior process. The angle between the horizontal branch and ascending branch of the quadratojugal is an obtuse angle, similar to that found in some late-diverging Titanosauriformes such as *Rapetosaurus krausei* (Rogers & Forster, 2004) and *Tapuiasaurus macedoi* (Wilson *et al.,* 2016). This differs from early-diverging Titanosauriformes such as *Euhelopus zdanskyi* and Brachiosauridae, indicating that mosaic evolution occurred in the skull of *Liaoningotitan sinensis*. The ratio of surangular dorsoventral height to angular dorsoventral height is 2.2. The dentary is U-shaped and robust, with a circular rostral side. The teeth are spoon-shaped with narrow crowns, and are only distributed in the anterior region of the premaxilla, maxilla, and dentary. The number of maxillary teeth is 9. The dental formula is Pm4+m9/d9, rostral convex to lateral and lingual concave to medial. The slender index of the teeth (the ratio of the tooth crown length to tooth crown width) is nearly 3.76. The cross-section of the crown is elliptical. The teeth had no rostral groove, lingual ridge, or serrations. The angle between the long axis of the tooth crown and the abrasive surface is approximately 30°. The ratio of the tooth crown and tooth root length is approximately 1.1.

Figure 3. Skull of *Liaoningotitan sinensis* holotype

Scale: 15 cm

Abbreviations: a, angulare; aof, antorbital fenestra; d, dentary; l, lacrimal; m, maxilla; n, nasal; o, orbit; pa, palatine; pt, pteroid; pm, premaxilla; qj, quadratojugal; sa, surangulare; t, teeth.

Cervical vertebrae: Only one anterior cervical vertebra and five posterior cervical vertebrae are well preserved, but the anterior and posterior surfaces, and prezygapophyses and postzygapophyses of the vertebrae are not visible. The anterior cervical vertebra is approximately 30 cm in length, with only the left surface visible. There is a shallow pleurocoel, which is isolated by a lamina on the lateral surface of the anterior cervical vertebra, similar to that in *Bellusaurus sui* (Mo, 2013). The diapophysis is triangular and connected to the caput tuberculum. The postcentroparaphyseal lamina connects the diapophysis to the postzygapophysis. The anterior cervical rib is a double head type. The posterior cervical vertebrae preserve the caput costae. The anterior cervical rib has a rib ridge.

Five interrelated, speculated, posterior cervical vertebrae are preserved, with lengths of approximately 8 cm, 18 cm, 26 cm, 17 cm, and 16 cm. All posterior cervical vertebrae are flat, presumably flattened by the rock bed. All neural arches and neural spines are incomplete. The diapophyses are triangular in shape. Only the last two vertebrae ribs are well preserved and are double head type.

Dorsal vertebrae: There are only two preserved posterior dorsal vertebrae, referred to as 'a' and 'b' for distinguishing. Both dorsal vertebrae are flat, also presumed to have been flattened by the rock bed. The angle between the spine and diapophysis is a right angle, with the spine projecting to the dorsal side. The parapophysis is approximately parallel with the diapophysis and vertical to the neural arch.

The left profile surface of dorsal vertebra 'a' is 11 cm long. The angle between the diapophysis and posterior centrodiapophyseal lamina is an acute angle. The diapophysis extends to the lateral and dorsal side, similar to that in *Liubangosaurus hei* (Mo, Xu & Buffetaut, 2010). The angular surface of the diapophysis and parapophysis is elliptical. The pneumatic foramen (pleurocoel) of the lateral surface is shallow, similar to that seen in Euhelopodidae (Mannion *et al.,* 2013).

The posterior angular surface of vertebra 'b' is opisthocoelous and wider than its height. The ratio of the mediolateral width to dorsoventral height of the centrum is 1.2, which is greater than that seen in *Daxiatitan binglingi* (You *et al.,* 2008) and less than that seen in *Mamenchisaurus youngi* (Ouyang, 2003). The length of the neural spine is shorter than the centrum. The diapophysis extends in a traverse orientation, and the location of the diapophysis is slightly lower than the hyposphene. The width of the vertebral foramen is greater than its length. The postzygapophysis, hyposphene, and centropostzygodiapophseal lamina are Y-shaped. The neural spine is not bifurcated, similar to that seen in Titanosauria (Mannion *et al.,* 2013). The spinopostzygapophyseal laminae are narrow and their lateral extension is not conspicuous. The ventral profile of the centra is incomplete, and the ratio of the dorsoventral height of the neural spine to posterior angular centrum is 0.98. The pneumatic foramen (pleurocoel) of the lateral surface is shallow and close to the dorsal margin, similar to that seen in Euhelopodidae and *Dongbeititan dongi* (Mannion *et al.,* 2013; Wang *et al.,* 2007).

Sacral vertebrae: Sacral vertebrae I, II, III (s1, s2, s3) are preserved, but embedded in the rock, so only the right sides are visible. All centra are amphiplatyan. The right lateral surface is visible with no neural arch, and the spine is preserved. S2 is well preserved, while s1 and s3 are fragmented. The left sacral yoke is preserved. The vertebrae are rectangular, with the anterior and posterior region being equal heights. There are no apparent concavities on the lateral surface of the vertebrae. All vertebrae are interrelated but have not fused, suggesting that this specimen was still in an immature stage at the time of death.

Caudal vertebrae: All caudal vertebrae are embedded in the rock, so only the left sides are visible. The middle and posterior caudal vertebrae are preserved and interrelated, but only one middle and two caudal vertebrae are completely preserved. They are all opisthocoelous. The left lateral surface is visible with no developed diapophyses or concavities. The ventral surface has visible concavities, with the concavity of the anterior caudal centrum being shallower than that of the posterior caudal centra. The neural arch is in the front region of the vertebra and extends in an upper posterior orientation. The angle between the arch and vertebra is approximately 25°. The prezygapophysis is long, extending to the anterior, beyond the vertebra. The distance the prezygapophysis extends beyond the anterior margin of the centrum in the middle posterior neural arches is 49% of the centrum length, similar to that seen in Somphospondyli. The postzygapophysis of the middle caudal vertebra approximately aligns with the posterior centrum. The angle between the spine and vertebra is approximately 60°. No chevron bones were preserved on the vertebrae.

Figure 4. Vertebrae of *Liaoningotitan sinensis* holotype

A. Anterior cervical vertebra. B. Posterior cervical vertebrae. C. Anterior dorsal vertebrae. D. Sacrum. E. Middle caudal vertebra. F. Posterior caudal vertebrae

Abbreviations: ar, arch; c, centra; cpol, centropostzygodiapophseal lamina; cr, cervical rib; di, diapophysis; hyps, hyposphene; pa, parapophysis; pcdl, posterior centrodiapophyseal lamina; pcpl, post centroparaphyseal lamina; pl, pleurocoel; poz, postzygapophysis; prz, prezygapophysis; s, sacrum; scy, sacral yoke; sp, spine; spol, spinopostzygapophyseal lamina

Scapula: The left and right scapulae are both preserved. The proximal end extends to the dorsal lateral. The dorsal side is thick, and the ventral side is thin. The proximal end is medially curved, similar to that in Somphospondyli. The ratio of the maximum dorsoventral height to the minimum dosorventral height of the scapular blade is 1.2 cm, less than that of *Dashanpusaurus dongi* (Ren, 2020) or *Jiangshanosaurus lixianensis* (Mannion *et al.,* 2019a). The scapula has a lateral ridge in the middle of the shaft that extends to the anterior and posterior, similar to that of *Jiangshanosaurus lixianensis* (Mannion *et al.,* 2019a), and speculated to be the attachment point of the subcoracoscapularis muscle. The ratio of the overall length of the scapular blade to its narrowest dorsoventral length is 5.06. The acromion process is not preserved. The posterior margin of the dorsal part of the acromial plate is concave. The angle between the acromion posterior region and the scapular shaft long axis is 37°. A subtriangular process located in the anteroventral corner of the scapular blade is the tuberosity, or attachment point, for the triceps brachii muscle, similar to that in *Yongjinglong datangi* (Li *et al.,* 2014). The stylolite of the scapula and coracoid is a nearly straight line, similar to that in *Ruyangosaurus giganteus* (Lv *et al.,* 2014). The angular surface of the coracoid is vertical to the long axis of the scapula. The glenoid cavity is elliptical shaped and medially curved, similar to that seen in Somphospondyli. The cross-section of the middle region of the scapular shaft is D-shaped. The thickest region of the shaft is located in the 1/3 region of the proximal end. The width of the proximal end is 38% of the overall length of the scapula. The dorsoventral height of the distal end is greater than the dorsoventral height of the proximal end and the dorsal side of the proximal end extends slightly to the dorsoventral and posterior side. The distal end extends to the dorsoposterior and posterior side, with an attachment point of the teres major muscle located on the lateral distal end of the scapula.

Humerus: Both the left and right humerus are well preserved. The humerus is short, with a length around 70% of the femur. Three surfaces of the proximal end are preserved, though incomplete. The middle and medial surface of the proximal end are lateral, similar to those in Mamenchisauridae (Yang, 2014). The proximal end is fan-shaped and its maximum width is 54% of the length of the humeral shaft and the minimum width of the proximal end is 31% of the length of the humeral shaft, which are both greater than in Brachiosauridae. The proximal end extends, indicating that the forelimb is robust. The lateral and medial surface of the humerus are asymmetric and the angle of the medial is sharper than the angle of the lateral. The slender index, or the ratio of the humerus length to the midshaft width of the humerus, is 4.4, which is less than that of *Fusuisaurus zhaoi* (Mo *et al.,* 2020). PHR, or the ratio of the length of the proximal end to the width of the midshaft, is 2.3, which is less than those of both *Ruyangosaurus giganteus* (Lv *et al.,* 2014) and *Notocolossus gonzalezparejasi* (Bernardo *et al.,* 2016). The humeral head is oval-sharped. The height of the proximal end and the humeral head is shorter than the height of the greater trochanter. The muscle scar located in the anterior middle region of the proximal end is speculated to be the attachment point of the coracobrachialis muscle. This muscle scar is flat rather than concave, dissimilar to the attachment point found in the same position in Mamenchisauridae, *Ruyangosaurus giganteus*, *Patagotitan mayorum* (Yang, 2014; Lv *et al.,* 2014; Carballido *et al.,* 2017), and other Titanosauriformes dinosaurs, indicating that this is an identifying characteristic of *Liaoningotitan sinensis*. The cross-section of the humeral shaft is elliptical. The humerus decreases in size from the proximal end to the distal end. The deltopectoral rest is robust, located in the 1/3 region of the shaft, and extends to the distal and medial profile surface, similar to that in Titanosauria and Lithostrotia (Mannion *et al.,* 2013). The length of the deltopectoral rest is 26% of the shaft's length, less than that seen in *Omeisaurus tianfuensis* and *Huangshanlong anhuiensis* (Ren, 2020). The deltopectoral rest is the attachment point of the pectoralis muscle. The concave shaft is not conspicuous, and is located in the medial side of the deltopectoral rest. The width of the distal end is 41% of the shaft length of the humerus. The narrowest width of the middle of the shaft is 54% of the distal end's widest measurement. The radial and ulnar condyles are well preserved, extending to the distal end, with a 51° angle. The ulnar condyle is slightly larger than the radial condyle. The anterior surface of the ulnar condyle is divided by a ridge, which differs from most Titanosauriformes dinosaurs, indicating that this is also an identifying characteristic of *Liaoningotitan sinensis*. The medial part of the ulnar condyle is greater than the lateral part. The robust index of the humerus, or the ratio of the average of the sum of the widest parts of the proximal end, middle, and distal end to the total length of the humeral shaft, is 0.38, which is greater than the 0.29 robust index of the humerus in *Qingxiusaurus youjiangensis*, (Mo *et al.,* 2008) and less than the 0.39 robust index of the humerus in

Zhuchengtitan zangjiazhuangensis (Mo *et al.,* 2017).
Radius: Only the left radius is preserved, which is 42 cm long, robust, and straight. The width of the proximal end is 25% of the total length. The cross-section of the middle of the shaft is elliptical. The lateral margin of the humerus does not bulge at the lateral side of the deltopectoral crest, dissimilar to that in *Qingxiusaurus youjiangensis* (Mo *et al.,* 2008), but similar to that in *Diamantinasaurus matildae* (Poropat *et al.,* 2014).
Ulna: Only the left ulna is preserved, is triradiate, and 53 cm in length. The width of the proximal end is 26 cm and the width of the distal end is 12 cm.
Forefoot: Only the right forefoot is preserved. Metacarpus I-IV (m1-4) and two phalanxes (p1 and p2) are preserved. The distal end of metacarpus I, II, and III extend, similar to a forefoot from an unnamed sauropod dinosaur excavated from the Tuchengzi Formation, Liaoning Province, China (Dong, 2001). The middle region of the metacarpus is thin. Phalanges III and IV are fused with the metacarpus. The length of the proximal end of metacarpus II is 27% of the overall length of metacarpus II. Metacarpus III is the longest. The length of all metatarsals is greater than their width. The medial surface of metacarpus IV is slightly concave. Phalanx 1 and phalanx 2 are covered by gypsum. Phalanx I has a robust claw, speculated to have been used for defending against carnivorous theropods or for attacking competitors during courtship.

Figure 5. Forelimbs of the *Liaoningotitan sinensis* holotype

A. Scapula. B. Humerus. C. Radius. D. Ulna. E. Forefoot

Scale: A-D: 50 cm. E: 15 cm

Abbreviations: c, claw; p, phalanx; dpc, deltopectoral rest; gl, glenoid cavity; hd, humerus head; ltr, lateral ridge.; m, metacarpus; ms, muscle scar; rac, radial condyle; s, stylolite; scb, scapular blade; stp, subtriangular process; tm, attachment point of muscle teres major; ulc, ulnar condyle.

Table 2. Humerus measurements in some Titanosauriformes

Ilium: The illium is approximately 70 cm in length and is not fused with the sacrum. The ilium is elliptical, is slightly concave in lateral view, and the dorsal side bulges into an arch, similar to that in

Analong chuanjieensis (Ren, 2020). The dorsoventral height of the ilium is 42% of the overall length of the ilium. The lateral side of the ventral surface bulges slightly. The preacetabular process extends to the anterior, and the anterior end is acute and triangular, which is different from that in *Qiaowanlong kangxii* (Li & You, 2009), *Dongyangosaurus sinensis* (Lv *et al.,* 2008), and *Ruyangosaurus giganteus* (Lv *et al.,* 2014), but similar to that in *Qinlingosaurus luonanmensis* (Xue *et al.,* 1996). The angle is 50°, which is less than that in *Qinlingosaurus luonanensis* (Xue *et al.,* 1996) and greater than that in *Dongyangosaurus sinensis* (Lv *et al.,* 2008), but similar to the angle seen in *Shunosaurus lii* (Zhang, 1988) and *Mamenchisaurus youngi* (Ouyang, 2003). The lateral side of the postactabular process is flat, unlike *Ruixinia,* which has a distinct bulge on the lateral side of the postactabular process (Mo *et al.,* 2022).

Pubis: The pubic bone is approximately 70 cm in length. The proximal end is plate-like and flat, and the shaft is not inflated. The acetabulum is semicircular. The pubic foramen is an elliptical shape. The pubic apron is located on the ventral aspect of the pubis. The length of the angular surface of the ilium is 19% of the pubis shaft's length.

Ischium: The ischium is approximately 70 cm in length, Y-shaped, and triradiate, similar to that in *Huanghetitan ruyangensis* (You *et al.,* 2006). The dorsoventral length of the proximal end is twice that of the distal end and is 57% of the overall length. The middle region of the proximal end is flat. The iliac process is triangular. The acetabulum is semicircular and conspicuously concave. The ratio of the dorsoventral width of the ischium's distal shaft to the ischium's proximodistal length is 0.24. The ratio of the anteroposterior length of the proximal plate to its total length is 0.67. The ratio of the dorsoventral width of the distal end of the ischial shaft to the smallest dorsoventral width of the shaft is 0.9, similar to that in Somphospondylans.

Figure 6. The right pelvic girdle of *Liaoningotitan sinensis* holotype

A. Ilium. **B**. Ischium. **C**. Pubis

Scale: 35 cm

Abbreviations: act, acetabulum; ilpeds, iliac peduncle; isped, ischial peduncle; obf,obturator formen. pa, public apron; pped, pubis peduncle; prap, preacetabular process.

Femur: The femur is 106 cm long. The width of the proximal end is 36 cm and the width of the distal end is 40 cm. The width of the proximal end is 27% of the total length of the femur. There is a distinct lateral bulge located at the lateral margin of the proximal end, similar to that in *Yunmenglong* and *Patagotitan mayorum* (Lv *et al.,* 2013; Carballido *et al.,* 2017). The femoral head is well developed and is confluent with the proximal end, lacking a distinct neck. The angle between the dorsal margin of the proximal end and the lateral margin is 127°. The shaft is long and robust with an elliptical cross-section. The *GI*, or the ratio of the femoral midshaft's minimum width to the total length of the femur, is 0.16, which is greater than that in *Daxiatitan binglingi* (You *et al.,* 2008) and *Ruyangosaurus giganteus* (Lv *et al.,* 2014), but less than that in *Dongbeititan dongi* (Wang *et al.,* 2007) and *Huabeisaurus allocotus* (Pang & Cheng, 2000). The greater trochanter is not conspicuously developed. The lateral process is located in the lower part of the greater trochanter and is 1/3 of the shaft's lateral dimension. In the distal end, the fibular and tibial condyles extend laterally and are concave. The *RI*, or the ratio of the sum of the widths of the proximal, middle, and distal ends to the total femur length, is 0.36. The medial margin of the femur is concave, similar to that in *Ruyangosaurus giganteus* (Lv *et al.,* 2014).

Tibia: The tibia length is 56% of the femur length. The proximal end extends. The tibial ridge is well developed and extends laterally to the 2/3 position of the shaft. The length of the ridge is 94% of the width of the tibial proximal end. The fibular angular surface is located behind the ridge and is concave. The 1/3 position of the tibia shaft extends. The narrowest position of the tibia is located below the middle point of the shaft, and is 1/3 of the width of the proximal end. The distal end extends to both the anterior and posterior. The second cnemial crest is absent, similar to that in Euhelopodidae. The narrowest region of the tibial shaft is located above the center point of the tibial shaft.

Fibula: The length of the fibula is slightly shorter than the length of the tibia and is half the length of the femur. The length of the proximal end of the fibula is 66% of the length of the proximal end of the tibia. The shaft of the fibula is straight and narrow with both medial and lateral shrinkage evident.

There is a tibial ligament muscle scar. The distal end of the fibula extends and is convex on the medial side. The ante process of the fibula is flat.

Hindfoot: The right hindfoot is preserved. Metatarsal I-IV (m1-4) and one phalanx (p) are preserved. The hindfoot has a developed, robust, and flat claw. The lateral and medial lateral sides of all metatarsal are curved. In metatarsal II to IV, the claws are regressed and the phalanges are fused with the metatarsal. Metatarsal I is robust and short, with a proximal end that extends slightly. The length of metatarsal I is 30% of its radius and 63% of the length of metatarsal II. The phalanx is robust. Metatarsal II is 20 cm long, and is distinctly longer and narrower than metatarsal I, similar to those in *Opisthocoelicaudia* and *Notocolossus* (Borsuk-Bialynicka,1977; Bernardo *et al.,* 2016). The width of the proximal end of metatarsal II is narrower than the distal end. The ratio of the length of metatarsal II to its radius is 0.2. Metatarsal III is the longest, but the ratio of the length of its proximal end to its radius is also 0.2. The lateral profile of metatarsal III is convex. The shaft of metatarsal IV is the thinnest one of the metacarpi. The width of its proximal end is equal to the width of its distal end. The ratio of the length of metatarsal IV to the radius is 0.1.

Figure 7. Hindlimbs of *Liaoningotitan sinensis* holotype

A. Femur. B. Fibula. C. Tibia. D. Hindfoot

Scale: A, B, C: 25 cm. D: 20 cm

Abbreviations: ap, ante process; c, claw; cc, cnemial crest; p, phalanx; fc, fibla condyle; gt, greater trochanter; h, head; interg, inter groove; lb, lateral bulge; m, metatarsal; tc, tibia condyle; tls, tibial ligament muscle scar.

Table 3. Femur measurements of some Titanosauriformes

Skull Reconstruction

The skull of the *Liaoningotitan sinensis* holotype has preserved premaxilla, maxilla, dentary, angulare, and supraangulare bones, partial quadratojugal bones, and some preserved teeth. An apparent slope is present between the premaxilla and maxilla, and the naris opens laterally. These characteristics are similar to those in *Mamenchisaurus youngi* (Ouyang, 2003), *Omeisaurus maoianus* (Tang *et al.,* 2001), and early-diverging Titanosauriformes such as *Euhelopus zdanskyi*

(Poropat & Benjamin, 2013). Therefore, *Mamenchisaurus youngi* and *Euhelopus zdanskyi* were used as references for the reconstruction of the coloboma nasal, premaxilla, maxilla, parietal, and frontal bones of *Liaoningotitan sinensis*. However, the quadratojugal of *Liaoningotitan sinensis* differs from that in *Mamenchisaurus youngi*, *Omeisaurus maoianus,* and *Euhelopus zdanskyi*. The angle between the horizontal branch and the ascending branch of the quadratojugal of *Mamenchisaurus youngi*, *Omeisaurus maoianus,* and *Euhelopus zdanskyi* is close to a right angle, but in *Liaoningotitan sinensis*, the angle between the horizontal branch and ascending branch of the quadratojugal is an obtuse angle. This characteristic is more similar to that of the late-diverging Titanosauriformes, such as *Nemegtosaurus mongoliensis* (Wilson, 2005), *Tapuiasaurus macedoi* (Wilson *et al.,* 2016), and *Rapetosaurus krausei* (Rogers & Forster*,* 2004), indicating that the skull of *Liaoningotitan sinensis* is in a transitional state in the evolution from the early-diverging Titanosauriformes to the late-diverging Titanosauriformes. Therefore, it is inferred that the postorbital bones of *Liaoningotitan sinensis* are similar to those of the late-diverging Titanosauriformes. These unusual characteristics revealed that mosaic evolution has occurred in the skull of *Liaoningotitan sinensis*. The result of the *Liaoningotitan sinensis* skull reconstruction is shown in Figure 8.

Figure 8. The reconstruction of the skull of *Liaoningotitan sinensis.* (The white part is the part missing from the holotype.)

Body Type Estimation

The *Xinjiangtitan shanshanensis* holotype was used for estimating the body length of the *Liaoningotitan sinensis* holotype because of its complete vertebrae sequences. The *Xinjiangtitan shanshanensis* holotype is a well-preserved sauropod dinosaur specimen, with complete cervical, dorsal, sacral, and caudal vertebrae, and a complete appendicular skeleton. It was unearthed from the Upper Jurassic Qigu Formation of Qiketai town, Shanshan County, Xinjiang, China, and was classified as a member of the Mamenchisauridae family (Zhang, 2019). The ratio of the length of the posterior vertebra to the length of the anterior vertebra (such as dorsal vertebra 2/dorsal vertebra 1) of the *Xinjiangtitan shanshanensis* holotype was calculated and then applied to the vertebrae of *Liaoningotitan sinensis*. The result indicated the total length of the *Liaoningotitan sinensis* holotype is approximately 13 m. The height of the scapula and the lengths of the humerus, ulna, metacarpus, and pes all indicate the *Liaoningotitan sinensis* specimen had a body length of approximately 13 m and a shoulder height of approximately 2 m (Fig 2). However, the sacral vertebrae of the *Liaoningotitan sinensis* holotype are not fused, indicating the holotype is an immature specimen, so the body of a mature *Liaoningotitan sinensis* was probably larger.

Phylogenetic Analysis

The first phylogenetic analysis of *Liaoningotitan sinensis* was performed in 2018, using a matrix modified from Wilson and Upchurch. The results showed that *Liaoningotitan sinensis* was from the Somphospondyli clade of Titanosauriformes, which is a sister group to Titanosauria (Zhou *et al.,* 2018). To further analyze the phylogenetic location of *Liaoningotitan sinensis*, this study used the matrix modified from Poropat *et al.,* 2023 in TNT 1.5 software for the phylogenetic analysis. *Liaoningotitan* was added as a genus to the matrix of Poropat *et al.,* 2023, which includes 126 taxa (OTUs) and 556 characteristics. Extended implied weighting (EIW) analyses were used with the following settings: max. trees was set to 150,000; tree bisection and reconnection (TBR) was used; new technology search was selected; random addition sequences were changed from 1 to 1,000 addseqs; sect search, ratchet, drift, and tree fusing were all used; K=12; and all other options were set to default. The results showed 18,928 most parsimonious trees, a tree length of 2,818, a CI of 0.208, and a RI of 0.581. Standard bootstrap with the number of replicates changed from 100 to 5,000 identified 11 unstable operational taxonomic taxa in the strict consensus tree: AODF 906, AODF 836, *Sarmientosaurus*, *Savannasaurus*, *Diamantinasaurus*, *Epachthosaurus*, *Normanniasaurus*, *Argentinosaurus*, *Mendozasaurus*, *Futalognkosaurus,* and *Puertasaurus*. Therefore, a reduced consensus tree analysis was then performed that excluded these 11 taxa. The final result identified *Liaoningotitan* within Euhelopodidae (see matrix in supplement).

Figure 9. Phylogenetic analysis reduced consensus tree of *Liaoningotitan sinensis* PMOL-AD00112 (red). Matrix from Poropat *et al.,* 2023. 1, Titanosauriformes. 2, Brachiosauridae. 3, Somphospondyli. 4, Euhelopodidae. 5, Titanosauria. 6, Lithostrotia.

Discussion

Four visible characteristics support the classification of *Liaoningotian sinensis* within Somphospondyli: (1) the scapular glenoid surface is deflected, facing both anteroventrally and medially; (2) the tibia lacks a ‘second cnemial crest’; (3) the ratio of the dorsoventral width across the ischial distal shaft to the proximodistal length of the ischium is 0.2 or greater; (4) the anterior margin of the centrum in the middle-posterior caudal neural arches is 20% or more of the centrum length (excluding the pal).

Three visible characteristics support the classification of *Liaoningotitan sinensis* within Euhelopodidae: (1) the dorsoventral height of the posterior dorsal neural spines divided by the posterior centrum dorsoventral height is less than 1.0; (2) the pneumatic foramen (pleurocoel) in the lateral surface of the dorsal centra is shallow; (3) the presence of the subtriangular process in the dorsoventral surface of the scapular blade (Mannion *et al.,* 2013).

Comparison between *Liaoningotita*n and other partial Somphospondylan holotypes in China from the Cretaceous Period:

Comparison between *Liaoningotitan* and *Dongbeititan*: Similarities between Dongbeititan and *Liaoningotitan* include a distinct bulge site at the lateral margin of the femur; the femoral head is confluent with the proximal end and has no developed neck; metatarsal I is shorter than metatarsal II-IV; and metatarsal II is narrower than metatarsal I. *Dongbeititan* differs from *Liaoningotitan* in the following ways: *Dongbeititan* has a broad pubis, with the distal end notably extending from the dorsoventral surface; the ischial peduncle of *Dongbeititan* is short, and the ischium is slightly longer than the pubis.

Comparison between *Liaoningotitan* and *Ruyangosaurus*: There are many differences between *Liaoningotitan* and *Ruyangosaurus*. The narrowest dorsoventral height of the *Ruyangosaurus* scapular blade is less than that in *Liaoningotitan*. The *RI* of the humerus of *Ruyangosaurus* is less than that of *Liaoningotitan*. In *Ruyangosaurus,* two of the distal condyles of the femur are the same size, but in *Liaoningotitan,* the fibular condyle is bigger than the tibial condyle at the distal end of the femur. The anterior region of the *Ruyangosaurus* ilium is circular, rather than the sharp anterior region present in the ilium of *Liaoningotitan*. The dorsoventral height of the ilium divided by the overall length of the ilium of *Ruyangosaurus* is greater than in *Liaoningotitan*. The *GI* of the *Ruyangosaurus* femur is less than that of the *Liaoningotitan* femur. The narrowest region of the tibial shaft of the *Ruyangosaurus* is behind the middle point of the tibial shaft, contrary to that in *Liaoningotitan*. The location of the cnemial crest of *Ruyangosaurus* is lower than in *Liaoningotitan*. The neural spine of the posterior dorsal vertebra of *Ruyangosaurus* is bifurcated. The pleurocoel of the dorsal vertebra of *Ruyangosaurus* is deeper than that of *Liaoningotitan*. *Ruyangosaurus* and *Liaoningotitan* have the following similarities: the stylolite between the scapula and coracoid is a straight line; the humeral deltopectoral crest extends to the medial surface; the proximal end of the scapula is curved inward; the ventral surface of the posterior dorsal vertebra is concaved (Lv *et al.,* 2014).

Comparison between *Liaoningotitan* and *Jiangshanosaurus*: These two taxa differ in many characteristics, such as the location of the diapophysis, which is lower than the hyposphere in *Jiangshanosaurus,* but aligned with the hyposphere in *Liaoningotitan*. The angle between the arch and the centrum, and the angle between the neural spine and the centrum of the middle-posterior caudal vertebra of *Jiangshanosaurus* are greater than those in *Liaoningotitan*. The pleurocoel of the dorsal vertebra of *Jiangshanosaurus* is noticeably deeper than in *Liaoningotitan*. *Jiangshanosaurus* and *Liaoningotitan* share the following similarities: the dorsal vertebrae are opisthocoelous, the pubis is flat, and the length of the neural arch is longer than the posterior caudal centrum (Mannion *et al.,* 2019a).

Comparison between *Liaoningotitan* and *Dongyangosaurus*: There are many differences between *Dongyangosaurus* and *Liaoningotian.* All the neural spines of the dorsal vertebrae of *Dongyangosaurus* are short and bifurcated, and the pleurocoel of the posterior dorsal vertebrae of *Dongyangosaurus* is deeper than that of the dorsal vertebrae of *Liaoningotitan*. The diapophysis of the posterior dorsal vertebrae in *Dongyangosaurus* is located at the caudodorsal of the parapophsis. The lateral view of the ilium of *Dongyangosaurus* is convex, contrary to that of *Liaoningotitan*. The anterior process of the ilium of *Dongyangosaurus* is blunt, and the anterior process of the ilium of *Liaoningotitan* is subtriangular. The pubis of Dongyangosaurus is shorter than its ischium, but the pubis and ischium are approximately equal in *Liaoningotitan*. *Dongyangosaurus* and *Liaoningotitan* do share some similarities, such as the slightly concave ventral side of the dorsal vertebrae and the short diapophyses with circular surfaces that extend laterally. The facets of the diapophysis are larger than the parapophysis in both *Dongyangosaurus* and *Liaoningotian*, and the shaft of the ischium in both dinosaurs is plate-like (Lv *et al.,* 2008).

Comparison between *Liaoningotitan* and *Yongjinglong*: There are many similar characteristics in *Liaoningotitan* and *Yongjinglong,* such as a medially-curved proximal end of the scapula and a D-shaped cross section of the scapula. In both *Liaoningotitan* and *Yongjinglong,* the tuberosity of the triceps brachii muscles is located in the ventral side of the anterior side of the proximal end of the scapula, and the attachment point of the teres major muscle is located in the distal end of the scapula blade. However, there are also many differences between *Liaoningotitan* and *Yongjinglong:* in *Yongjinglon,* the ventral side of the distal end of the scapula extend to the posterior, contrary to that in *Liaoningotitan,* and the dorsal and ventral sides of the scapular blade of *Yongjinglong* are approximately parallel (Li *et al.,* 2014).

Comparison between *Liaoningotitan* and *Euhelopus*: *Liaoningotitan* and *Euhelopus* have many similar characteristics, such as the narial fenestra in the skull opening laterally and the slope present in the anterior surface of the maxilla. In both *Liaoningotitan* and *Euhelopus,* the maxilla is part of the antorbital fossa, and the dorsoventral height of the posterior dorsal neural spines divided by the posterior centrum dorsoventral height is less than 1.0. The subtriangular process at the anteroventral corner of scapular blade is speculated to be the tuberosity of the triceps brachii muscles in both taxa, which is also similar to *Yongjinglong*. The following differences are present between *Liaoningotitan* and *Euhelopus*: the dentition of *Euhelopus* extends to the posterior of the mouth and aligns with the anterior side of the antorbital fenestra, while the dentition of *Liaoningotitan* is limited to the anterior of the mouth; the anterior centrodiapophyseal lamina in the posterior dorsal vertebra of *Euhelopus* is well-developed and forms a K shape with the posterior centrodiapophyseal lamina and posterior centroparapophyseal lamina, but the posterior dorsal vertebra of *Liaoningotitan* is not conspicuous (Poropat & Benjamin, 2013; Wilson & Upchurch, 2010).

Comparison between *Liaoningotitan* and *Huabeisaurus*: There are many similarities between *Liaoningotitan* and *Huabeisaurus,* such as an opisthocoelous dorsal vertebra with a convex ventral side. Both *Liaoningotitan* and *Huabeisaurus* have a pleuroceol located on the lateral side of dorsal vertebra. The neural arch of the caudal vertebra site in the anterior region of the neural spine of the dorsal vertebra is not bifurcated in either dinosaur, and both have a scapular shaft that is medially curved. *Liaoningotitan* and *Huabeisaurus* have a shallow concavity located between the two distal condyles of the humerus, and both dinosaurs have a distinct lateral bulge on the femur. There are also many differences between *Liaoningotitan* and *Huabeisaurus:* the scapula of *Huabeisaurus* has no distinct subtriangular process; the preacetabular process of *Huabeisaurus* extends and is circular, differing from the triangular preacetabular process of the ilium of *Liaoningotitan* (D'Emic *et al.,* 2013; Pang & Cheng, 2000).

Other Cretaceous Titanosauriformes in China

The result of this analysis indicates that most genera of Cretaceous Titanosauriformes in China fit within Somphospondyli. *Liubangosaurus* was first considered a non-Titanosauriformes Eusauropoda dinosaur (Mo, Xu & Buffetaut, 2010), then classified into Lithostrotia (Mannion *et al.,* 2013) or Euhelopodidae (Poropat *et al.,* 2014), and finally classified into Euhelopodidae again in the present analysis. *Yongjinglong*, *Qiaowanlong*, *Euhelopus,* and *Gobititan* have been classified into Euhelopodidae in many analyses (Mannion *et al.,* 2019b; Poropat *et al.,* 2023), and *Qiaowanlong* was considered a Brachiosaurus in an initial genus construction paper (Li & You, 2009); the results of the present analysis support the classification of these genera into Euhelopodidae. *Dongbeititan* is classified as a non-Titanosauria Somphospondylan in the present analysis, which aligns with the results of previous analyses (Mannion *et al.,* 2019b; Poropat *et al.,* 2014), *Jiangshanosaurus* was classified as non-Euhelopodidae and Titanosauria Somphospondylan in the present analysis, but has been classified into Euhelopodidae and Lithostrotia in past analyses (Mannion *et al.,* 2013; Poropat *et al.,* 2023). In the present analysis, *Huanghetitan liujiaxiaensis,* and *Huanghetitan ruyangensis* are non-Euhelopodidae and Titanosauria Somphospondylan; and *Baotianmansaurus*, *Huabeisaurus*, *Dongyangosaurus*, *Daxiatitan*, *Xianshanosaurus*, *Ruyangosaurus,* and *Mongolosaurus* are Titanosauria. In past analyses, *Mongolosaurus* has been classified as Lithostrotian, and *Ruyangosaurus*, *Dongyangosaurus* and *Jiangshanosaurus* have been identified as non-Titanosauria Somphospondylans (Poropat *et al.,* 2014; Mannion *et al.,* 2019a). The results of the present analysis support *Xianshanosaurus* constituting a sister group with *Daxiatitan,* and *Dongyangosaurus* constituting a sister group with *Huabeisaurus*.

About Euhelopodidae

The present analysis supports the validity of Euhelopodidae. In this analysis, Euhelopodidae include *Euhelopus*, *Qiaowanlong*, *Erketu*, *Yongjinglong*, *Liubangosaurus*, *Tangvayosaurus*, *Gobititan*, *Phuwiangsaurus,* and *Liaoningotitan*. Fossil evidence has shown that the earliest taxon of Euhelopodidae in Asia is *Euhelopus*, from the Berriasian period of China (Han *et al.,* 2024). In addition, the present analysis identified *Australodocus*, *Astrophocaudia,* and *Tastavinsaurus* as taxa of Euhelopodidae, indicating the distribution region of Euhelopodidae might not limited to Asia. In the present analysis, *Liaoningotitan* constitutes a monophyletic group with all taxon of Euhelopodidae in Asia except *Liubangosaurus*. These conclusions will have to be verified in the future as fossil evidence continues to accumulate. The results of this analysis support the sister group in *Tangvayosaurus* and *Phuwiangosaurus*. *Liaoningotitan*, *Yongjinglong*, *Euhelopus*, *Gobititan*, *Liaoningotitan*, *Qiaowanlong*, *Erketu*, *Tangvayosaurus*, *Phuwiangosaurus*, and *Liubangosaurus* indicate that Euhelopodidae was a large and diverse taxon in Asia during the Cretaceous Period.

The Titanosauriformes Skull

The current understanding of the evolution of the skull of Titanosauriformes is lacking. As of July 2024, only 10 taxa of Titanosauriformes have been found with complete skulls (dentary and teeth included): *Giraffatitan*, *Abydosaurus*, *Euhelopus*, *Liaoningotitan*, *Malawisaurus*, *Tapuiasaurus*, *Sarmientosaurus*, *Diamantinasaurus*, *Nemegtosaurus,* and *Rapetosaurus*. Except Giraffatitan, all of these taxa are from the Cretaceous Period, with *Abydosaurus*, *Euhelopus*, *Liaoningotitan*, *Malawisaurus*, and *Tapuiasaurus* coming from the Early Cretaceous. No individuals have been found from the Turonian-Campanian interval, making research on Titanosauriformes difficult (Paul, 1988; Wilson & Sereno, 1988; Daniel *et al.,* 2010; Poropat & Benjamin, 2013; Zhou *et al.,* 2018; Gomani, 2005; Wilson *et al.,* 2016; Martinez *et al.,* 2016; Poropat *et al.,* 2023; Wilson, 2005; Rogers & Forster, 2004).

Based on the 10 taxa that have been found, Titanosauriformes skulls can be divided into three types: (1) In the first type, the snout is taller than the back of the skull (the nasal area bulges), all or most part of narial fenestra is visible in lateral view, and the angle between the horizontal and ascending branches of the quadratojugal is a right or acute angle, such as in *Giraffatitan*, *Abydosaurus*, *Euhelopus,* and *Malawisaurus*, and similar to the skulls of *Mamenchisaurus* and *Camarasaurus* (Daniel *et al.,* 2010; Poropat & Benjamin, 2013; Zhou *et al.,* 2018; Gomani, 2005; Ouyang, 2003). (2) This type has a shorter snout compared to the back of the skull (nasal area is low), less of the narial fenestra is visible in lateral view, the skull is elongated in lateral view, and the angle between the horizontal and ascending branches of the quadratojugal is an obtuse angle, such as in *Tapuiasaurus*, *Nemegtosaurus* and *Rapetosaurus,* and similar to the skull of *diplodocus* (Wilson *et al.,* 2016; Wilson, 2005; Rogers & Forster, 2004). (3) The skulls of *Sarmientosaurus* and *Diamantinasaurus* have a combination of characteristics of Titanosauriforme types 1 and 2. These have an elongated skull, with a nasal area taller than the back of skull, a low narial fenestra, and an acute angle between the horizontal and ascending branches of the quadratojugal. These characteristics indicate that mosaic evolution occurred in the skull of *Sarmientosaurus* and *Diamantinasaurus*, and they are transitional species in the evolution of Titanosauriformes. *Liaoningotitan* has a bulging nasal area and an obtuse angle between the horizontal and ascending branches of the quadratojugal, therefore mosaic evolution also occurred in the skull of *Liaoningotitan* and it is also a transitional species, but differs from *Sarmientosaurus* and *Diamantinasaurus*, (Martinez *et al.,* 2016; Poropat *et al.,* 2023; Zhou *et al.,* 2018).

The Autapomorphic Analysis of *Liaoningotitan*

The ratio of skull height (no mandibula): length, ulna length: humerus length ratio, and tibia length: femur length ratio were all calculated. To determine whether these ratios were autapomorphic characteristics, other Eusauropod taxa were added to the analysis, as shown in Table 4.

Table 4. Eusauropod taxa added to the autapomorphic analysis of skull height: length, ulna length: humerus length, and tibia length: femur length ratios

The Skull Height: Length Ratio

The ratio of the skull height to the skull length was approximately 0.2 in *Liaoningotitan*. For testing whether this ratio was autapomorphically higher than in other Eusauropod dinosaurs, an ordinary least squares regression of $\log_{10}$ (skull height: cm, no mandibula) against log10 (skull length: cm) was performed for 20 Eusauropod taxa (10 Titanosauriformes and 10 non-Titanosauriformes taxa) using Past4.0 and the following linear regression equation:

$$\log_{10}(\text{skull height}) = 1.03\log_{10}(\text{skull length}) - 0.332$$

Confidence intervals (95%) of the slope of $\log_{10}$ (skull length) were 0.82 to 1.41. Confidence intervals of the Y intercept were -0.95 to 0.03. The result was close to the skull height: skull length ratio of *Diamantinasaurus*, a Titanosaur, indicating this ratio is not an autapomorphic characteristic in *Liaoningotitan* (Figure 10).

Figure 10. Skull height: skull length ratio in Eusauropoda. Linear regression (deep red line) and 95% confidence intervals (deep blue lines) show *Liaoningotitan* has a high skull height to length ratio, approaching that of *Omeisaurus tianfuensis*, *Mamenchisaurus jingyanensis*, *Diamantinasaurus,* and *Nemegtosaurus*.

The Ulna Length: Humerus Length Ratio of *Liaoningotitan*

The ratio of ulna length to humerus length is approximately 0.71 in *Liaoningotitan*. For testing whether the ratio was autapomorphically higher than in other Eusauropod dinosaurs, an ordinary least squares regression of log10 (ulna length) against log10 (humerus length: cm) was performed for 20 Eusauropod taxa (10 Titanosauriformes and 10 non-Titanosauriformes taxa), using the following linear regression equation:

$$\log_{10}(\text{ulna length}) = 0.82\log_{10}(\text{humerus length}) + 0.194$$

Confidence intervals (95%) of the slope of $\log_{10}$ (humerus length) were 0.66 to 1.13. Confidence intervals of the Y intercept were -0.43 to 0.52. The results indicated that the ulna length: humerus length ratio of *Mamenchisaurus youngi*, *Omeisaurus maoianus*, *Klamelisaurus,* and *Yuzhoulong* were close to that of

Liaoningotitan, but because these are non-Titanosauriformes Eusauropods, distantly related to *Liaoningotitan*, the ulna length to humerus length ratio was considered an autapomorphic trait in *Liaoningotitan* (Figure 11).

Figure 11. Ulna length: humerus length ratio in Eusauropoda. Linear regression (deep red line) and 95% confidence intervals (deep blue lines) show *Liaoningotitan* has a low ulna to humerus length ratio, close to that of *Omeisaurus maoianus*, *Mamenchisaurus youngi*, *Klamelisaurus,* and *Yuzhoulong*.

The Tibia Length: Femur Length Ratio of *Liaoningotitan*

The ratio of the length of the tibia to that of the femur is approximately 0.56 in *Liaoningotitan*. For testing whether the ratio was autapomorphically higher than in other Eusauropod dinosaurs, ordinary least squares regression of $\log_{10}$ (tibia length: cm) against log10 (femur length: cm) was performed for 20 Eusauropod taxa (10 Titanosauriformes and 10 non-Titanosauriformes taxa), using the following linear regression equation:

$$\log_{10}(\text{tibia length}) = 0.98\log_{10}(\text{femur length}) - 0.179$$

Confidence intervals (95%) of the slope of $\log_{10}$ (femur length) were 0.77 to 1.14. Confidence intervals of the Y intercept were -0.50 to 0.28. The results indicated that some non-Titanosauriformes Eusauropods have similar tibia length: femur length ratios as *Liaoningotitan*. However, non-Titanosauriformes Eusauropods are only distantly related to *Liaoningotitan*, so the ratio of tibia length to femur length was considered an autapomorphic trait in *Liaoningotitan* (Figure 12).

Figure 12. Tibia length: femur length ratio in Eusauropoda. Linear regression (deep red line) and 95% confidence intervals (deep blue lines) show *Liaoningotitan* has a low tibia length to femur length ratio, similar to distantly related *Shunosaurus lii*, *Mamenchisaurus youngi*, *Yuzhoulong qurenensis,* and *Dashanpusaurus dongi*.

Conclusion

The *Liaoningotitan sinensis* holotype is a partial skeleton from the Lower Cretaceous Yixian Formation of Liaoning Province, China. It displays some characteristics that suggest *Liaoingotitan sinensis* is a valid species that can be distinguished from other Titanosauriformes dinosaurs. This analysis classifies *Liaoningotitan sinensis* into Euhelopodidae, indicating that Euhelopodidae dinosaurs inhabited the Jehol Biota, which increases the known diversity of sauropod dinosaurs in the Jehol Biota. The analysis results indicated that both the ulna length to humerus length ratio and the tibia length to femur length ratio were autapomorphic characteristics in *Liaoningotitan*, but the skull height to skull length ratio was not.

Acknowledgements

Thank you to the Paleontological Museum of Liaoning, Shenyang normal university for their research help and thank you to Professors Hu dongyu and Xing lida for their assistance.

REFERENCES

Bernardo J Gonzalez R, Lammana MC, David LDO, Carvo JO, Coria JP. 2016. A gigantic new dinosaur from the Argentina and the evolution of the Sauropod hind foot. SCIENTIFIC REPORTS 1-15 doi: 10.1038/srep19165.

Borsuk-Bialynicka, M. 1977. A new camarasaurid sauropod *Opisthocoelicaudia skarzynskii* gen. n., sp. n. from the Upper Cretaceous of Mongolia. *Palaeontol* Pol. 37, 5–63.

Carballido JL, Diego P, Alejandro O, Cerda IA, Salgado L, Garrido A C, Ramezani J, Cuneo NR, Krause JM. 2017. A new giant titanosaur sheds light on body mass evolution among sauropod dinosaurs. The Royal Society 1-10.

Calvo, J. O. 2014. New fossil remains of *Futalognkosaurus dukei* (Sauropoda, Titanosauria) from the Late Cretaceous of Neuquén, Argentina in *4th International Palaeontological Congress*. *The History of Life: A View from the Southern Hemisphere abstract volume*

(ed Cerdeño, E.) 325 (International Palaeontological Association)

Gilmore CW. 1946. Reptilian fauna of the North Horn Formation of central Utah. U.S.D.I. Prof. Pap. 210-C. 1–53.

Dai H, Tan C, Xiong Can, Ma, QY, Li N, Yu HD, Wei ZY, Wang P, Yi J, Wei GB, You HL, Ren XX. 2022. New macronarian from the Middle Jurassic of Chongqing, China: phylogenetic and biogeographic implications for neosauropod dinosaur evolution. ROYAL SOCIETY OPEN SCIENCE 9: 220794. https: //doi.org/10.1098/rsos.220794.

Daniel CB, Wilson JA. 2010. First complete sauropod dinosaur skull from the Cretaceous of the Americas and the evolution of sauropod dentition. Naturwissenschaften 97:379–391 DOI 10.1007/s00114-010-0650-6

D'Emic M, Mannion PD, Upchurch P, Benson RBJ, Pang QQ, Cheng ZW. 2013. Osteology of *Huabeisaurus allocotus* (Sauropoda: Titanosauriformes) from the Upper Cretaceous of China. PLoS ONE 8(8): e69375 doi: 10.1371/journal.pone.0069375.

Dong ZM. 2001. A forefoot of Sauropod from the Tuchengzi Formation of Chaoyang area in Liaoning, China. Proceeding of the English Annual Meeting of the Chinese Society of Vertebrae Paleontology. Beijing: Ocean Press.

Gomani EM. 2005. Sauropod dinosaurs from The Early Cretaceous of Malawi, Africa. Palaeontologia Electronica 8(1): 1-37.

Han FL, Yang L, Lou FS, Corwin S, Xu X, Qiu WF, Liu HF, Yu J, Wu R, Ke YZ, Xu MY, Hu JF, Lu PK. 2024. A new titanosaurian sauropod, *Gandititan cavocaudatus* gen. et sp. nov., from the Late Cretaceous of southern China. Journal of Systematic Palaeontology 22: 1, 2293038 doi: 10.1080/14772019.2023.2293038.

He XL, Li K, Cai KJ. 1988. *Omeisaurus tianfuensis*. Chengdu: Sichuan Scientific and Technologic Press.

Jiang S, Li F, Peng GZ, Ye Y. 2011. A New species of *Omeisaurus* from The Middle Jurassic of Zigong, Sichuan. VERTEBRATA PALASLATICA 49 (2): 185-194 doi: 10.19615/j. cnki. 1000-3118. 2011. 02. 004.

Janensch W. 1961. Die Gliedmaszen und Gliedmaszengurtel der Sauropoden der Tendaguru-Schichten. Palaeontographica Suppl. 7, 177–235.

Lacovara K, Lammana M, Lucio MI, Poole JC, *et al.,* 2014. A Gigantic, Exceptionally Complete Titanosaurian Sauropod Dinosaur from Southern Patagonia, Argentina. Scientific Reports doi: 10.1038/srep06196.

Li DQ, You HL. 2009. The first well-preserved Early Cretaceous Brachiosaurid dinosaur in Asia. Proceedings of the Royal Society B Biological Science 276: 4077-4082.

Li LG, Li DQ, You HL, Dodsen P. 2014. A New Titanosauria Sauropod from the Hekou Group (Lower Cretaceous) of the Lanzhou-Minhe Basin, Gansu Province, China. PLoS ONE, 9: e85979.

Lv JC, Li SX, Ji Q, Wang GF, Zhang JH, Dong ZM. 2006. New Eusauropod Dinosaur from Yuanmou of Yunnan

Province, China. ACTA GEOLOGICA SINICA 80(1): 1-10.
Lv JC, Pu HY, Xu L, Jia SH, Zhang JM, Shen CZ. 2014. *Osteology of giant sauropod dinosaur Ruyangosaurus giganteus Lv et al.* Beijing: Geological Press.
Lv JC, Xu L, Jiang XJ, Jia SH, Li M, Yuan CX, Zhang XL, Ji Q. 2009. A preliminary report on the new dinosaurian fauna from the Cretaceous of the Ruyang Basin, Henan Province of central China. Journal of the Paleontological Society of Korea 25(1): 43-56.
Lv JC, Xu L, Zhang XL, Pu HY. 2007. A New Gigantic Sauropod Dinosaur with the Deepest Known Cavity from the Cretaceous of China. Acta Geologica Sinica 81: 167-176.
Lv JC, Xu L, Zhang XL, Pu HY, Zhang YY, Jia SH, Chang HL, Zhang JM, Wei XF. 2013. A new sauropod dinosaur (Dinosauria, Sauropoda) from the late Early Cretaceous of the Ruyang Basin (central China). Cretaceous Research 1-12.
Lv JC, Yi LP, Zhong H, Wei XF. 2013. A New Somphospondylan Sauropod (Dinosauria, Titanosauriformes) from the Late Cretaceous of Ganzhou, Jiangxi Province of Southern China. ACTA GEOLOGICA SINICA (English Edition) 87(3): 678-685.
Lv JC, Yoichi, Cheng RJ, Zheng WJ, Jin XS, 2008. A New Titanosauriformess Sauropod from the Early Late Cretaceous of Dongyang Zhejiang Province. Acta Geologica Sinica 82: 225-235 doi: 10.1111/j.1755-6724.2008.tb00572.x.
Mannion PD. 2011. A reassessment of Monglosaurus haplodont, Gilmore, 1933, a Titanosaurian sauropod dinosaur from the Early Cretaceous of Inner Mongolia, People’s Republic of China. Journal of Systematic Paleontology 9(3): 355-378.
Mannion PD, Otero A. 2012. A Reappraisal of the Late Cretaceous Argentinean Sauropod Dinosaur *Argyrosaurus superbus*, with a Description of a New Titanosaur Genus. The Society of Vertebrate Paleontology 32(3): 614–638.
Mannion PD, Upchurch P, Barnes RN, Mateus O. 2013. Osteology of the Late Jurassic Portuguese sauropod dinosaur *Lusotitan atalaiensis* (Macronaria) and the evolutionary history of basal titanosauriforms. *Zoological Journal of the Linnean Society* 168, 98–206.
Mannion PD, Upchurch P, Jin Xin-sheng, Zheng WJ. 2019a. New information on the Cretaceous sauropod

dinosaurs of Zhejiang Province China: impact on Laurasian Titanosauriformes phylogeny and biogeography. Royal Society Open Science 1-22 doi: http: //dx.doi.org/10.1098/rsos.191057

Mannion P D, Upchurch P, Schawarz D, Wings O. 2019b. Taxonomic affinities of the putative titanosaurs from the Late Jurassic Tendaguru Formation of Tanzania: phylogenetic and biogeographic implications for eusauropod dinosaur evolution. Zoological Journal of Linnean Society 185: 784-905.

Marpamann JS, Carballido JL, Sander PM, Knotschke N. 2015. Cranial anatomy of the Late Jurassic dwarf sauropod *Europasaurus holgeri* (Dinosauria: Camarasauromorpha): ontogenetic changes and size dimorphism. Journal of Systematic Paleonotology 13(3): 221-263. doi: 10.1080/14772019. 2013. 875074.

Martinez RD, Lamman MC, Novas FE, Ridgely CR, Casal GA, Martínez JE, Vita JR, Witmer LM. 2016. A Basal Lithostrotian Titanosaur (Dinosauria: Sauropoda) with a Complete Skull: Implications for the Evolution and Paleobiology of Titanosauria. PLoS ONE 11(4): e0151661. doi:10.1371/journal. pone.0151661.

Mo JY, Fu QY, Yu YL, Xu X. 2023. A New Titanosaurian Sauropod from the Upper Cretaceous of Jiangxi Province, Southern China. Historical Biology, DOI: 10.1080/08912963.2023.2259413.

Mo JY, Xu X, Buffetaut E. 2010. A New Eusauropod dinosaur from the Lower Cretaceous of: Guangxi Province, Southern China. Acta Geologica Sinica (English edition). 84: 1328-1335.

Mo JY, 2013. *Bellusaurus sui*. Topics in Chinese dinosaurs paleontology. Zhengzhou: Henan Scientific and Technical Press 1-155.

Mo JY, Huang CL, Zhao ZR, Wang W, Xu X. 2008. A NEW TITANOSAUR (DINOSAURIA: SAUROPODA) FROM THE LATE CRETACEOUS OF GUANGXI CHINA. Vertebrata Palasiactia 46: 147-156.

Mo JY, Li JC, Ling YC, Buffetaut E, Suteethorn S, Varavudh S, Tong HY, Gilles CG, Romain AG, Xu X. 2020. New fossil remains of *Fusuisaurus zhaoi* (Sauropoda: Titanosauriformes) from the Lower Cretaceous of Guangxi China. HAL open science 1-7 doi: 10.1016/j.cretres.2020.104379.

Mo JY, Ma FM, Yu YL, Xu X. 2022. A New Titanosauriform Sauropod with An Unusual Tail from the Lower Cretaceous of Northeastern China. Journal Pre-proof. 1-51 https: //doi.org/10.1016/j.cretres.2022.105449.

Mo JY, Wang KB, Wang PY, Chen SQ, Xu X. 2017. A New Titanosauria Dinosaur from Late Cretaceous of Shandong. Geological Bulletin of China 1502-1505.

Moore AJ, Upchurch P, Barrett PM, Clark JM, Xu X. 2020. Osteology of *Klamelisaurus gobiensis* (Dinosauria, Eusauropoda) and the evolutionary history of Middle–Late Jurassic Chinese sauropods. Journal of Systematic Palaeontology 18(21): 1-95. doi: 10.1080/14772019.2020.1759706.

Otero A, Carballido JL, Moreno PA. 2020. The appendicular osteology of *Patagotitan mayorum* (Dinosauria, Sauropoda). Journal of Vertebrate Paleontology doi: 10.1080/02724634.2020.1793158.

Ouyang H. 2003. Skeletal Characteristics of *Mamenchisaurus youngi* and the Systematics of Mamenchisaurids. Chengdu: Chengdu Technical University 1-176.

Pang QQ, Cheng ZW. 2000. A New Sauropod Dinosaur from the Late Cretaceous of Tianzhen Shanxi Province China. Acta Geologica Sinica 74: 2-9.

Paul GS. 1988. The brachiosaur giants of the Morrison and Tendaguru With a description of a new subgenus, *Giraffatitan*, and a comparison of the world's largest dinosaurs. Hunteria Societas Paleonotographica Goloradensis ISSN No. 0892-3701.

Poropat SF, Benjamin PK. 2013. Photographic Atlas and Three-Dimensional Reconstruction of the Holotype Skull of *Euhelopus zdanskyi* with Description of Additional Cranial Elements. PLoS ONE 8: 1-17 doi: 10.1371/journal.pone.0079932.

Poropat SF, Kundrat M, Mannion PD, Upchurch P, Tischler TR, Elliott DA. 2021. Second specimen of the Late Cretaceous Australia sauropod dinosaur *Diamantinasaurus matildae* provides new anatomical information on the skull and neck of early titanosaurs. *Zoological Journal of the Linnean Society* 192, 610–674.

Poropat SF, Upchurch P, Mannion PD, Hocknull SA, Benjamin PK, Trish S, George HKS, Elliott D. 2014. Revision of the sauropod dinosaur Diamantinasaurus matildae Hocknull et al. 2009 from the mid-Cretaceous of Australia: Implications for Gondwanan titanosauriform dispersal. Gondwana Research 27 (2015) 995–1033.

Ren XX. 2020. Early evolution of sauropod dinosaurs based on new discovery and restudy of Chinese Middle Jurassic specimens. Beijing: University of Chinese Academic Science 1-295.

Ren XX, Jiang S, Wang XR, Peng GZ, Ye Y, King L, You HL. 2022. Osteology of *Dashanpusaurus dongi* (Sauropoda: Macronaria) and new evolutionary evidence from Middle Jurassic Chinese sauropods. Journal of Systematic Palaeontology 20: 1, 2132886 doi: 10.1080/14772019.2022.2132886.

Rogers KC, Forster RCA. 2004. The skull of *Rapetosaurus krausei* (Sauropoda: Titanosauria) from the Late

Cretaceous of Madagascar. The Society of Vertebrate Paleontology 24: 121-144 doi: 10.1671/A1109-10.

Rogers KC. 2009. The postcranial osteology of *Rapetosaurus krausei* (Sauropoda: Titanosauria) from the Late Cretaceous of Madagascar. Journal of Vertebrate Paleonotology 29(4): 1046-1086.

Salgado L, Gallina PA, Crabajal P. 2014. Redescription of *Bonatitan reigi* (Sauropoda: Titanosauria), from the Campanian-Maastrichtian of the Río Negro Province (Argentina). Historical Biology 27: 5, 525-548 doi: 10.1080/08912963.2014.894038.

Sekiya T. 2010. Re-examination of *Chuanjiesaurus anaensis* (Sauropoda, Dinosauria) from the Chuanjie Formation (Middle Jurassic) in Lufeng of Yunnan, China. Changchun: Jilin University, 1-95.

Smith JB, Lammana MC, Lacovara KJ, Dodsen P, Smith JR, Poole JC, Giegengack R, Attia Y. 2001. A Giant Sauropod Dinosaur from an Upper Cretaceous Mangrove deposit in Egypt. *Science* 292 (5522), 1704-1706. doi: 10.1126/science.1060561.

Tang F, Jin XS, Kang XM, Zhang GJ. 2001. *Omeisaurus maoianus* A complete Sauropoda from Jingyan, Sichuan. Beijing: Ocean Press.

Upchurch P, Mannion PD, Barret PM. 2011. Sauropod dinosaurs. Palaeontological Association 476-525.

Wang XL, Bandeira KLN, Qiu R, Jiang SX, Cheng X, Ma YX, Kellner AWA. 2021. The first dinosaurs from the Early Cretaceous Hami Pterosaur Fauna, China. Scientific reports (2021) 11: 14962 doi: https: //doi.org/10.1038/s41598-021-94273-7.

Wang XR, You HL, Gao CL, Cheng XD, Liu JY, 2007. *Dongbeititan dongi* the first Sauropod Dinosaur from the Lower Cretaceous Jehol Group of Western Liaoning Province China. Acta Geologica Sinica 6: 911-916.

Wang XR, Wu WH, Li T, Ji Q, Li YX, Guo JF. 2019. A new titanosauriform dinosaur (Dinosauria: Sauropoda) from Late Jurassic of Junggar Basin, Xinjiang. GLOBAL GEOLOGY 3(38): 1-8 doi: 10. 3969 /j. issn. 1004-5589. 2019. 03. 001.

Wilson JA. 2005. Redescription of Mongolia sauropod *Nemegtosaurus mongoliensis* Nowinskyi (Dinosauria: Saurichia) and Comments on Late Cretaceous Sauropod Diversity. Journal of Systematic Paleontology 3: 283-318.

Wilson JA, Diego P, Carvalho AB, Hussam Z. 2016. The skull of the Titanosaur *Tapuiasaurus macedoi* (Dinosauria: Sauropoda) a basal titanosaur from the lower Cretaceous of Brazil. Zoological Journal of Linnean

Society 178 611-662.

Wilson JA, Sereno P. 1998. Early Evolution and Higher-Level Phylogeny of Sauropod Dinosaurs. Society of Vertebrate Paleontology doi: 10.1080/02724634.1998.10011115

Wu WH. 2006. A new Sauropod dinosaur (*Jiutaisaurus*) from Cretaceous in Jiutai of Jilin, China. Changchun: Jilin University, 1-41.

Wilson JA, Upchurch P. 2010. Redescription and reassessment of the phylogenetic affinities of the *Euhelopus zdanskyi* (Dinosauria: Sauropoda) from the Early Cretaceous of China. Journal of Systematic Paleonotology 7:2, 199-239.

Xu X, Zhang XH, Tan QW, Zhao XJ, Tan L. 2006. A New Titanosaurian from Late Cretaceous of Nei Mongol, China. ACTA GEOLOGICA SINICA 80(1): 20-26.

Xue XX, Zhang YX, Bi Y, Yue LP, Chen DL. 1996. *The Development and Environmental Changes of the Intermontane Basins in the Eastern Part of Qinling Mountains*. Beijing: Geological Press.

Yang CY. 2014. The Phylogenetic evolution of Mamenchisauridae. Chengdu: Chengdu technical University. 1-172.

You HL, Tang F, Luo ZX. 2003. A new basal titanosaur (Dinosauria: Sauropoda) from the Early Cretaceous of China. Acta Geologica Sinica 77(4): 424-429.

You HL, Li DQ, Zhou LQ, Ji Q. 2006. *Huanghetitan liujiaxiaensis*: A New Sauropod Dinosaur from Hekou Group of Lower Cretaceous in Lanzhou Basin Gansu China. Geological Review 52: 669-674.

You HL, Li DQ, Zhou LQ, Ji Q. 2008. *Daxiatitan binglingi*: a Giant Sauropod Dinosaur from The Early Cretaceous of China. Gansu Geology 17: 2-10.

You HL, Ji Q, Lamanna MC, Li JL, Li YX. 2004. A Titanosaurian Sauropod Dinosaur with Opisthocoelous Caudal Vertebrae from the Early Late Cretaceous of Liaoning Province, China. ACTA GEOLOGICA SINICA 78(4): 907-911.

Zhang LJ. 2020. Analysis on fossil community of tetrapods in Lujiatun bed of Lower Cretaceous Yixian Formation in Beipiao, Liaoning. Global Geology 39: 738-744.

Zhang XQ. 2019. Study on *Xinjiangtitan shanshanensis* from the Late Jurassic of Shanshan, Xinjiang. Beijing: China University of Geoscience (Beijing) 1-314.

Zhang XL, Lv, JC, Xu L, Li JH, Yang L, Hu WY, Jia SH, Ji Q, Zhang CJ. 2009. A New Sauropod Dinosaur From the Late Cretaceous Gaogou Formation of Nanyang, Henan Province. ACTA GEOLOGICA SINICA 83(2): 212-221.

Zhang YH. 1988. THE MIDDLE JURASSIC DINOSAUR FAUNA FROM DASHANPU ZIGONG SICHUAN: SAUROPOD DINOSAURS (I): SHUNOSAURUS. Chengdu: Sichuan Technological Press.

Zhang YH, Li K, Zeng QH. 1998. A new species of Sauropod dinosaur from The Upper Jurassic of Sichuan Basin, China. Journal of Chengdu University of Technology 25(1): 62-70.

Zhou CF, Wu WH, Sekiya, Dong ZM. 2018. A New Titanosauriformes dinosaur from Jehol Biota of western Liaoning China. Global Geology 37: 328-333 doi: 10.3969/j.issn.1004-5589.2018.02.001.

Table 1(on next page)

Titanosauriformes in China (adapted from Han *et al.*, 2024)

Liaoningotitan sinensis	Beipiao County Liaoning Province Yixian Formation Early Cretaceous	Euhelopodidae (This study)	Zhou *et al.,* 2018
Dongbeitian dongi	Beipiao County Liaoning Province Yixian Formation Early Cretaceous	Somphospondyli	Wang *et al.,* 2007
Ruixinia zhangi	Beipiao County Liaoning Province Yixian Formation Early Cretaceous	Titanosauria	Mo *et al.,* 2022
Boreaolosaurus wimani	Beipiao County Liaoning Province Sunjiawan Formation Late Cretaceous	Saltasauridae	You *et al.,* 2004
Jiutaisaurus xidiensis	Changchun city Jilin Province Quantou Formation Late Cretaceous	Titanosauriformes	Wu, 2006
Huabeisaurus allocotus	Tianzhen County Shanxi Province Huiquanpu Formation Late Cretaceous	Non-Lithostrotia Titanosauria	Pang & Cheng, 2000
Euhelopus zdanskyi	Mengyin City Shandong Province Mengyin Formation Early Cretaceous	Euhelopodidae	Poropat & Benjamin, 2013
Zhuchengtitan zangjiazhuangensis	Zhucheng City Shandong Province Wangshi Group Late Cretaceous	Saltasauridae	Mo *et al.,* 2017
Sonidosaurus saihangaobiensis	Erenhot City Inner Mongolia Autonomous Region Erlian Formation Late Cretaceous	Titanosauria	Xu *et al.,* 2006
Mongolosaurus haplodon	Erenhot City Inner Mongolia Autonomous Region On gong Formation Early Cretaceous	Titanosauria	Mannion, 2011

Gobititan shenzhouensis	Subei County Gansu Province Xinminpu Group Early Cretaceous	Euhelopodidae	You, Tang & Luo, 2003
Yongjinglong datangi	Yongjing County Gansu Province Hekou Group Early Cretaceous	Euhelopodidae	Li *et al.,* 2014
Daxiatitan binglingi	Linxia Autonomous District Gansu Province Hekou Group Early Cretaceous	Titanosauria	You *et al.,* 2008
Qiaowanlong kangxii	Subei County Gansu Province Xinminpu Group Early Cretaceous	Euhelopodidae	Li & You, 2009
Huanghetitan liujiaxiaensis	Linxia Autonomous District Gansu Province Hekou Group Early Cretaceous	Somphospondyli	You *et al.,* 2006
Hamititan xinjiangensis	Hami City Xinjiang Autonomous Region Shengjinkou Formation Early Cretaceous	Somphospondyli	Wang *et al.,* 2021
Fushanosaurus qitaiensis	Qitai County Xinjiang Autonomous Region Shishigou Formation Late Jurassic	Titanosauriformes	Wang *et al.,* 2019
Silutitan sinensis	Hami City Xinjiang Autonomous Region ShengjinKou Formation Early Cretaceous	Euhelopodidae	Wang *et al.,* 2021
Ruyangosaurus giganteus	Ruyang County Henan Province Haoling Formation Early Cretaceous	Somphospondyli	Lv *et al.,* 2014
Huanghetitan ruyangensis	Ruyang County Henan Province Haoling Formation Early Cretaceous	Somphospondyli	Lv *et al.,* 2007
Xianshanosaurus shijiagouensis	Ruyang County	Lithostrotia	Lv *et al.,* 2009

	Henan Province Haoling Formation Early Cretaceous		
Yunmenglong ruyangensis	Ruyang County Henan Province Haoling Formation Early Cretaceous	Euhelopodidae	Lv *et al.,* 2009
Baotianmansaurus henanensis	Neixiang County Henan Province Gaogou Formation Late Cretaceous	Non-Lithostrotia Titanosauria	Zhang *et al.,* 2009
Qinlingosaurus luonanensis	Luonan County Shaanxi Province Shanyang Formation Late Cretaceous	Titanosauria	Xue *et al.,* 1996
Dongyangosaurus sinensis	Zhejiang Province Fangyan Formation Late Cretaceous	Non-Lithostrotia Titanosauria	Lv *et al.,* 2008
Jiangshanosaurus lixianensis	Zhejiang Province Jinhua Formation Early Cretaceous	Somphospondyli	Tang *et al.,* 2001
Gandititan cavocadatus	Ganzhou City Jiangxi Province Zhoutian Formation Late Cretaceous	Titanosauria	Han *et al.,* 2024
Jiangxititan ganzhouensis	Ganzhou City Jiangxi Province Nanxiong Formation Late Cretaceous	Titanosauria	Mo *et al.,* 2023
Gannansaurus sinensis	Ganzhou City Jiangxi Province Nanxiong Formation Late Cretaceous	Euhelopodidae	Lv *et al.,* 2013
Fusuisaurus zhaoi	Fusui County Guangxi Autonomous Region Napai Formation Early Cretaceous	Titanosauriformes	Mo *et al.,* 2006
Qingxiusaurus youjiangensis	Nanning City Guangxi Autonomous Region Red bed Late Cretaceous	Titanosauria	Mo *et al.,* 2008

Liubangosaurus hei	Fusui County Guangxi Autonomous Region Napai Formation Early Cretaceous	Titanosauriformes	Mo, Xu & Buffetaut, 2010

1

Table 2(on next page)

Humerus measurements in some Titanosauriforme

Species	proximal end length (mm)	Width midshaft (mm)	PHR	References
Liaoningotitan sinensis	400	170	2.35	This paper
Notocolossus gonzalezparejasi	720	255	2.88	Bernado *et al.*, 2016
Patagotitan mayorum	560	270	2.07	Otero *et al.,* 2020
Fusuisaurus zhaoi	565	215	3.07	Mo *et al.,* 2020
Ruangosaurus giganteus (referred)	540	320	1.68	Lv *et al.,* 2014
Rapetosaurus krausei	203	86	2.36	Rogers, 2009
Paralititan stromeri	562	234	2.40	Smith *et al.,* 2001
Futalognkosaurus dukei	600	250	2.40	Calvo *et al.,* 2014
Dreadnoughtus schrani	740	320	2.31	Lacovara *et al.,* 2014
Qingxiusaurus youjiangensis	370	155	2.38	Mo *et al.,* 2008

1

Table 3 (on next page)

Femur measurements of some Titanosauriformes

Species	Midshaft minimum length (mm)	Femur total length (mm)	GI	Reference
Liaoningotitan sinensis	230	1060	0.16	This paper
Dongbeititan dongi	230	1100	0.20	Wang *et al.,* 2007
Daxiatitan binglingi	300	1770	0.16	You *et al.,* 2008
Ruyangosaurus giganteus (referred)	300	1670	0.17	Lv *et al.,* 2014
Patagotitan mayorum	360	2360	0.15	Otero *et al.,* 2020
Yunmenglong ruyangensis	360	1920	0.18	Lv *et al.,* 2013
Opisthocoelicaudia skarzynskii	250	1395	0.17	Borsu-Bialynickak, 1977
Fushanosaurus qitaiensis	550	1800	0.31	Wang *et al.,* 2019
Huabeisaurus allocotus	245	1560	0.15	D'Emic *et al.,* 2013
Rapetosaurus krausei	177	657	0.26	Rogers, 2009

Table 4(on next page)

Eusauropod taxa added to the autapomorphic analysis of skull height: length, ulna length: humerus length, and tibia length: femur length ratios

Taxa	References
Shunosaurus lii	Zhang, 1988
Mamenchisaurus youngi	Ouyang, 2003
Mamenchisaurus jingyanensis	Zhang *et al.,* 1998
Omeisaurus tianfuensis	He *et al.,* 1988
Omeisaurus maoianus	Tang *et al.,* 2001
Omeisaurus jiaoi	Jiang *et al.,* 2011
Abrosaurus dongpoi	Yang, 2014
Bellusaurus sui	Mo, 2013
Nigersaurus taqueti	Upchurch *et al.,* 2011
Diplodocus	Upchurch *et al.,* 2011
Camarasaurus lentus	Upchurch *et al.,* 2011
Europasaurus holgeri	Marpamann *et al.,* 2015
Giraffatitan brancai	Paul, 1988; Janensch, 1961
Abydosaurus mcintoshi	Daniel *et al.,* 2010
Euhelopus zdanskyi	Poropat & Benjamin, 2013
Liaoningotitan sinensis	Zhou *et al.,* 2018; This paper
Malawisaurus dixeyi	Gomani, 2005
Diamantinasaurus matildae	Poropat *et al.,* 2014; 2023
Sarmientosaurus musacchioi	Martinez *et al.,* 2016
Tapuiasaurus macedoi	Wilson *et al.,* 2016
Nemegtosaurus mongoliensis	Wilson, 2005
Rapetosaurus krausei	Rogers & Forster, 2004; 2009
Dongbeititan dongi	Wang *et al.,* 2007
Ruyangosaurus giganteus	Lv *et al.,* 2014
Ruixinia zhangi	Mo *et al.,* 2022
Dreadnoughtus schrani	Lacovara *et al.,* 2014
Argyrosaurus superbus	Mannion & Otero, 2012

Elaltitan lillioi	Mannion & Otero, 2012
Alamosaurua sanjuanensis	Gilmore, 1946
Opisthocoelicaudia skarzynskyii	Borsuk-Bialynicka,1977
Patagotitan mayorum	Otero *et al.,* 2020
Huabeisaurus allocotus	D'Emic *et al.,* 2013
Bonatitan reigi	Salgado *et al.,* 2014
Dashanpusaurus dongi	Ren *et al.,* 2022
Yuzhoulong qurenensis	Dai *et al.,* 2023
Yuanmousaurus jiangyiensis	Lv *et al.,* 2006
Klamelisaurus gobiensis	Moore *et al.,* 2020
Chuanjiesaurus anaensis	Sekiya, 2010
Xinjiangtitan shanshanensis	Zhang, 2019

Figure 1

Geographic provenance of *Liaoningotitan sinensis* (Zhou *et al.*, 2018). Holotype locality of *Liaoningotitan sinensis* (indicated by red point in left map and green sign in right picture arrow) in Liaoning province, China; Left map copy

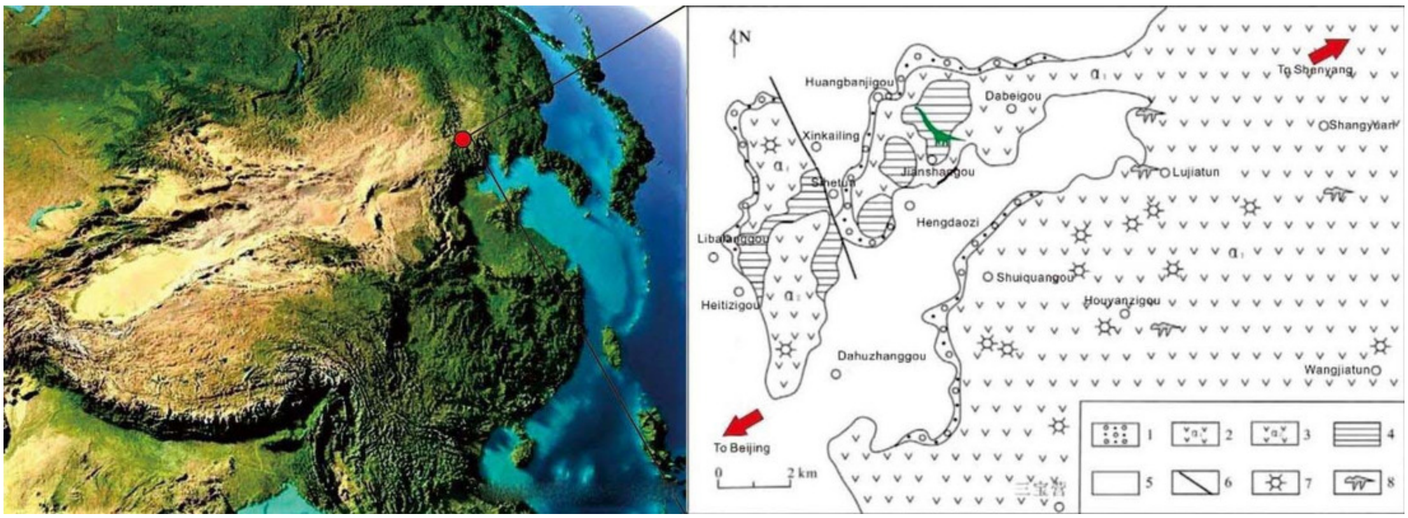

Figure 2

Reconstruction of *Liaoningotitan sinensis* (in left lateral view. Preserved elements of the holotype PMOL-AD00112 in green. Adapted from Bernardo *et al.*, 2016)

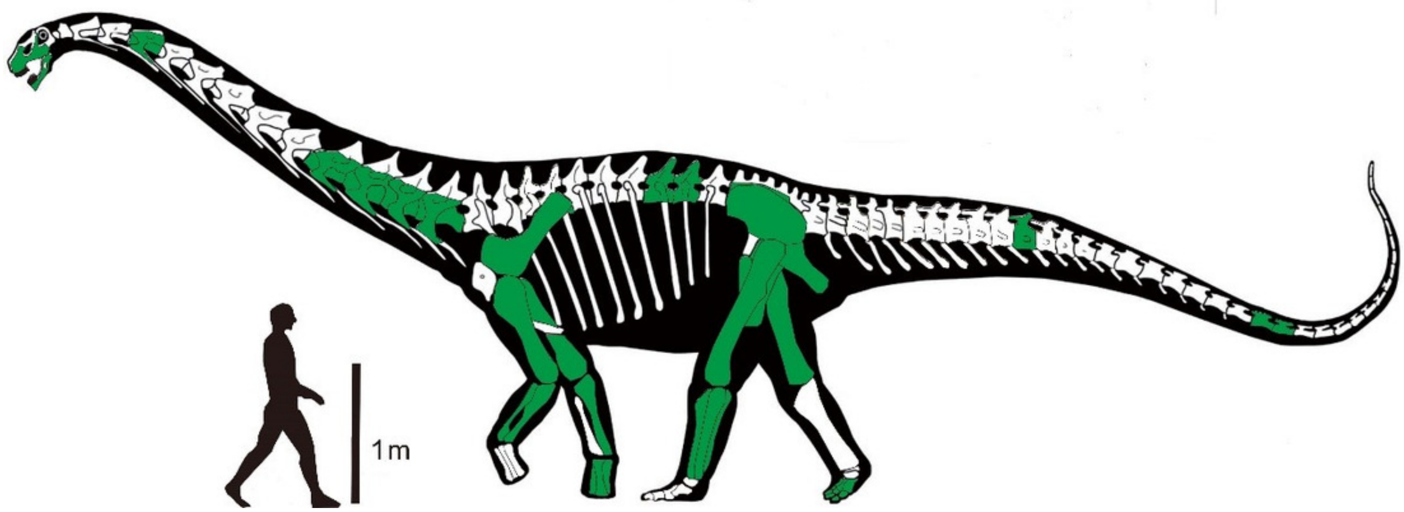

Figure 3

Skull of *Liaoningotitan sinensis* holotype

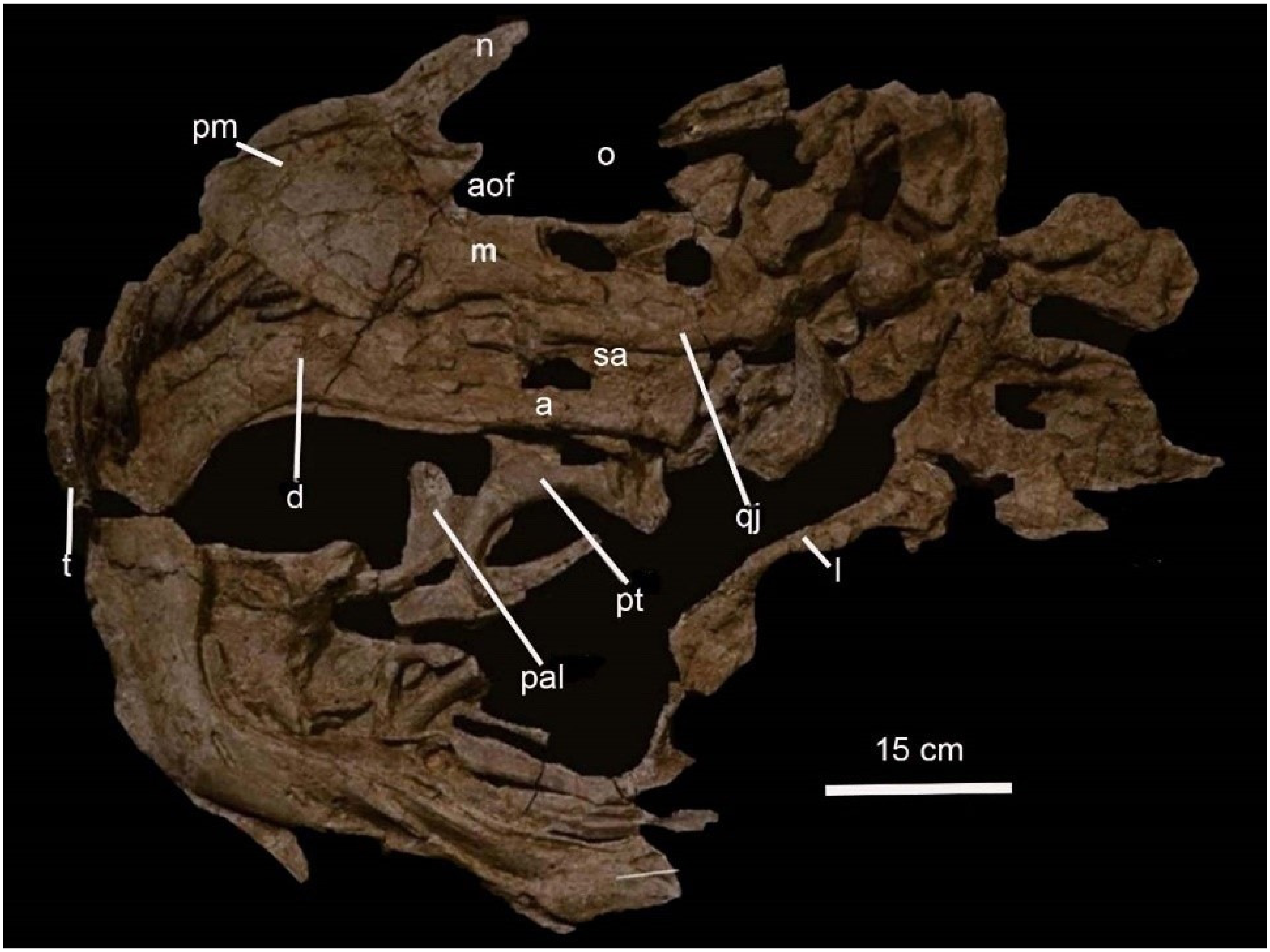

Figure 4

Vertebrae of *Liaoningotitan sinensis* holotype

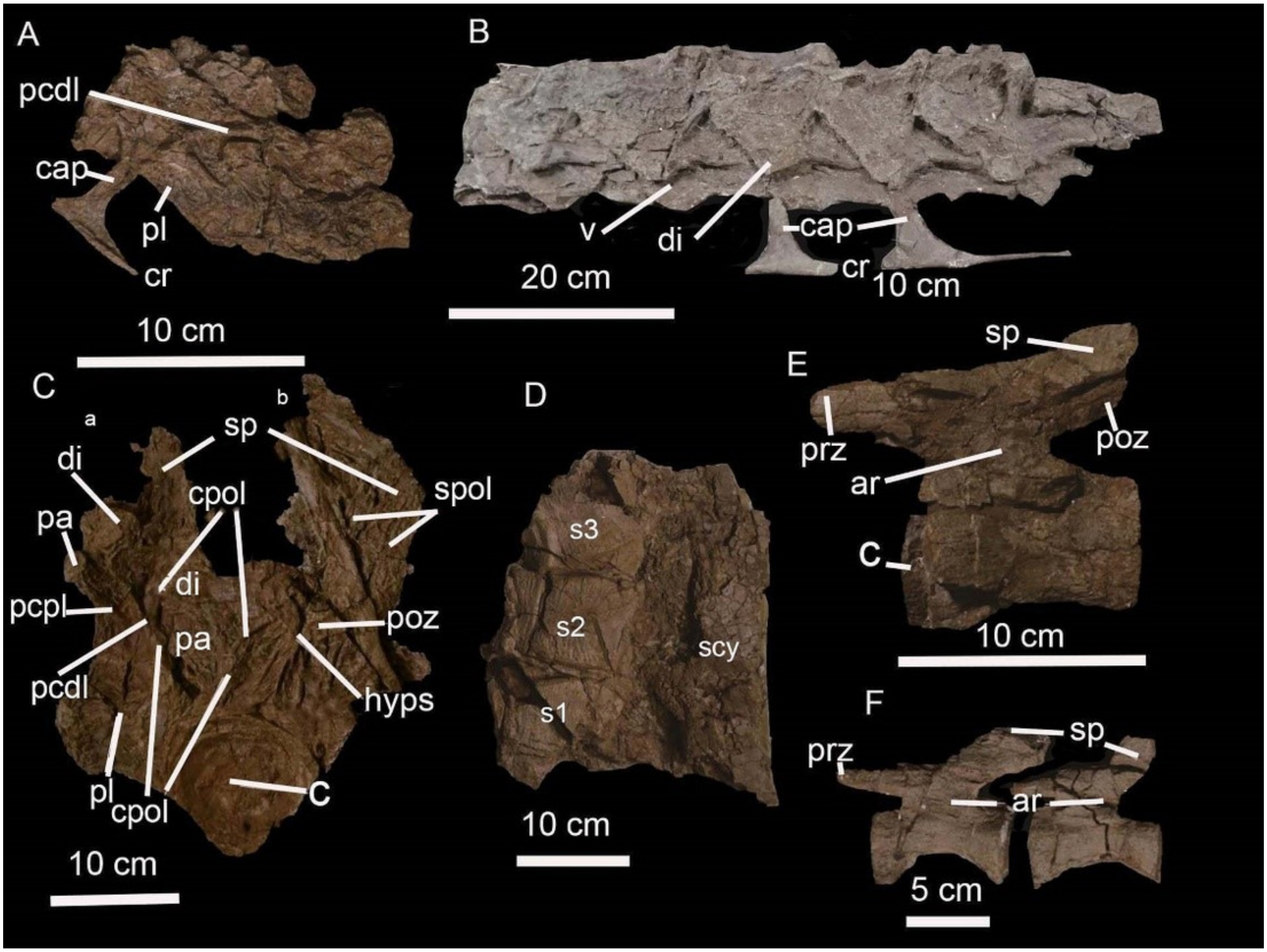

Figure 5

Forelimbs of the *Liaoningotitan sinensis* holotype

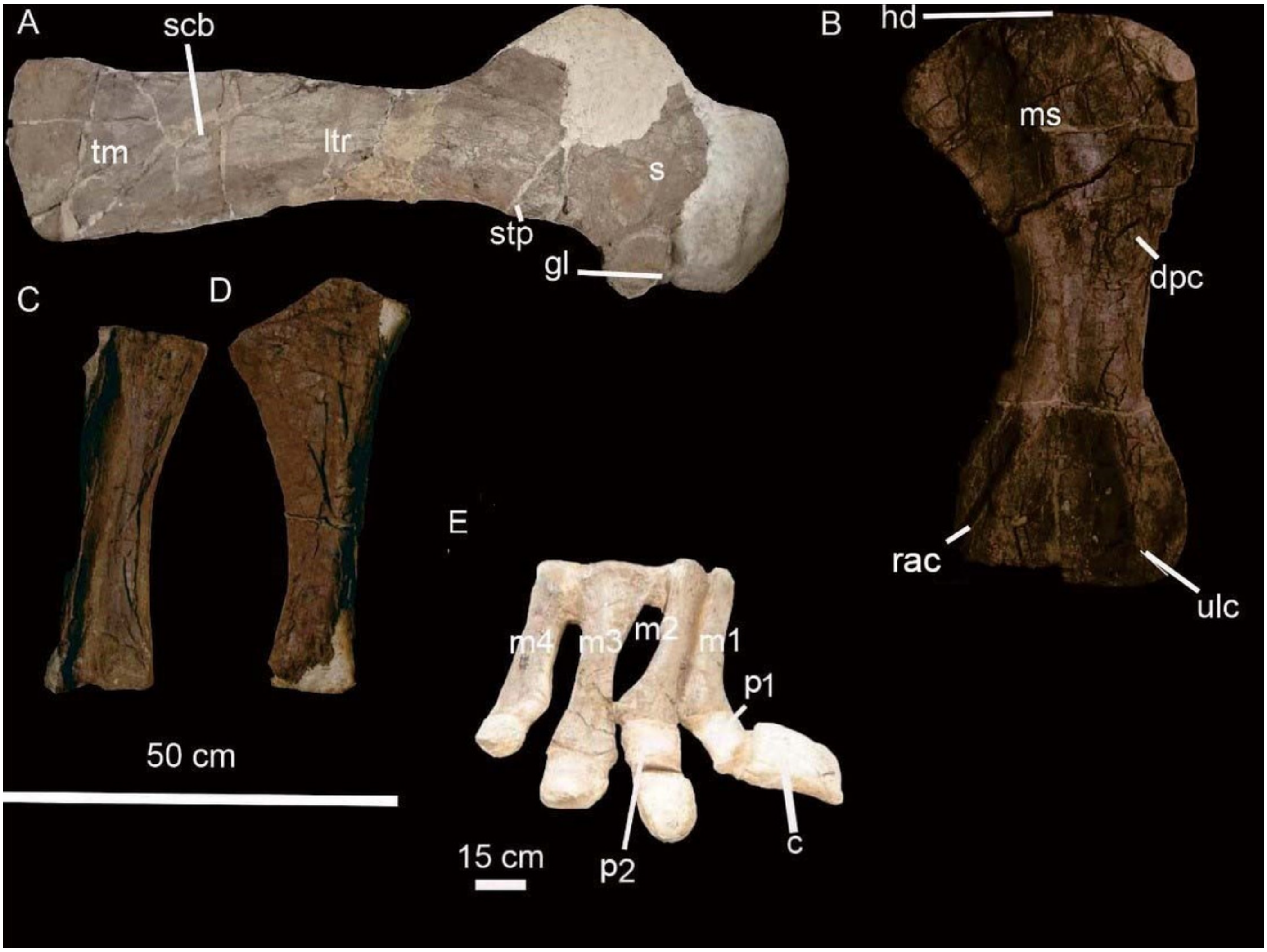

Figure 6

The right pelvic girdle of *Liaoningotitan sinensis* holotype

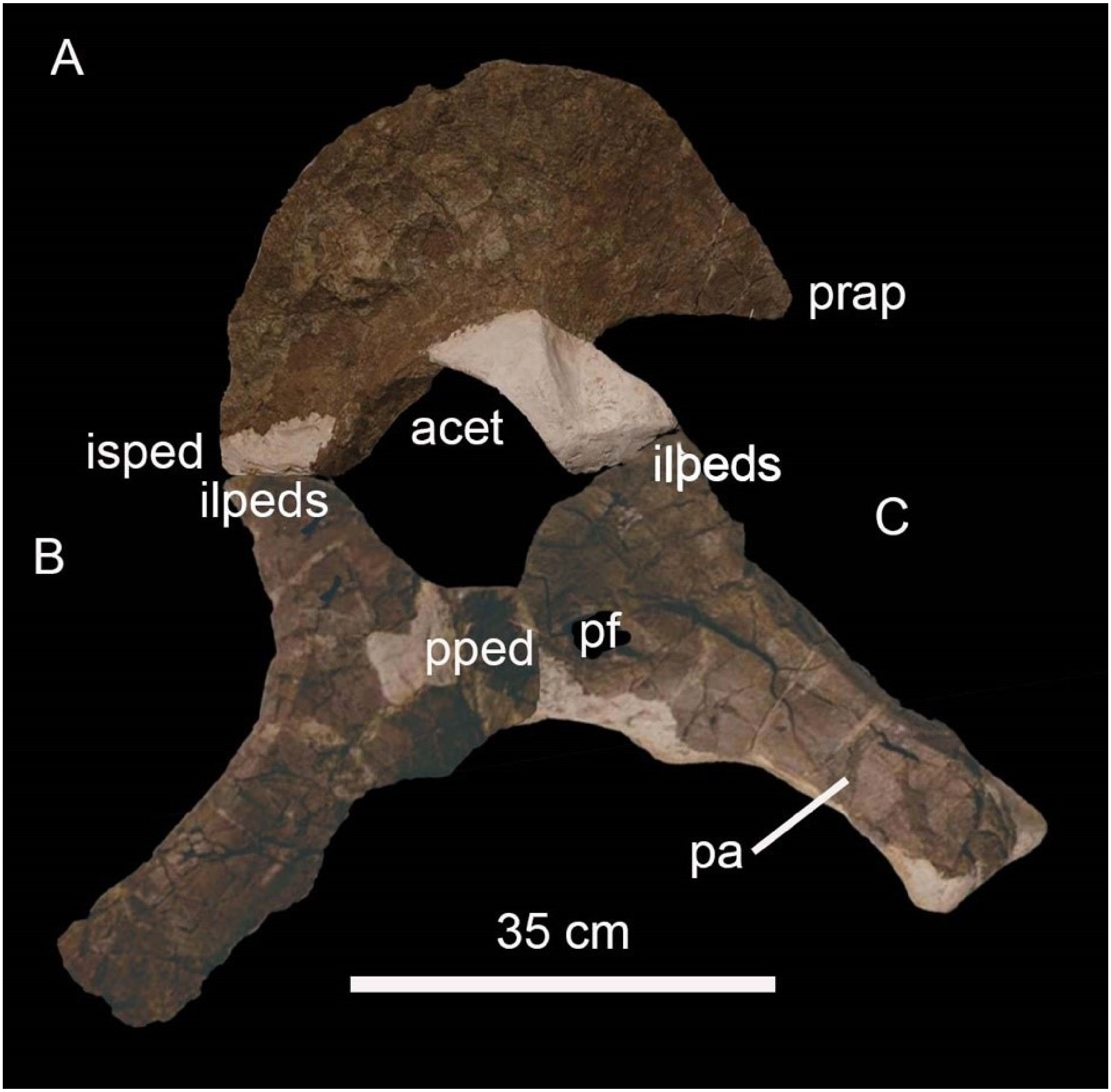

Figure 7

Hindlimbs of *Liaoningotitan sinensis* holotype

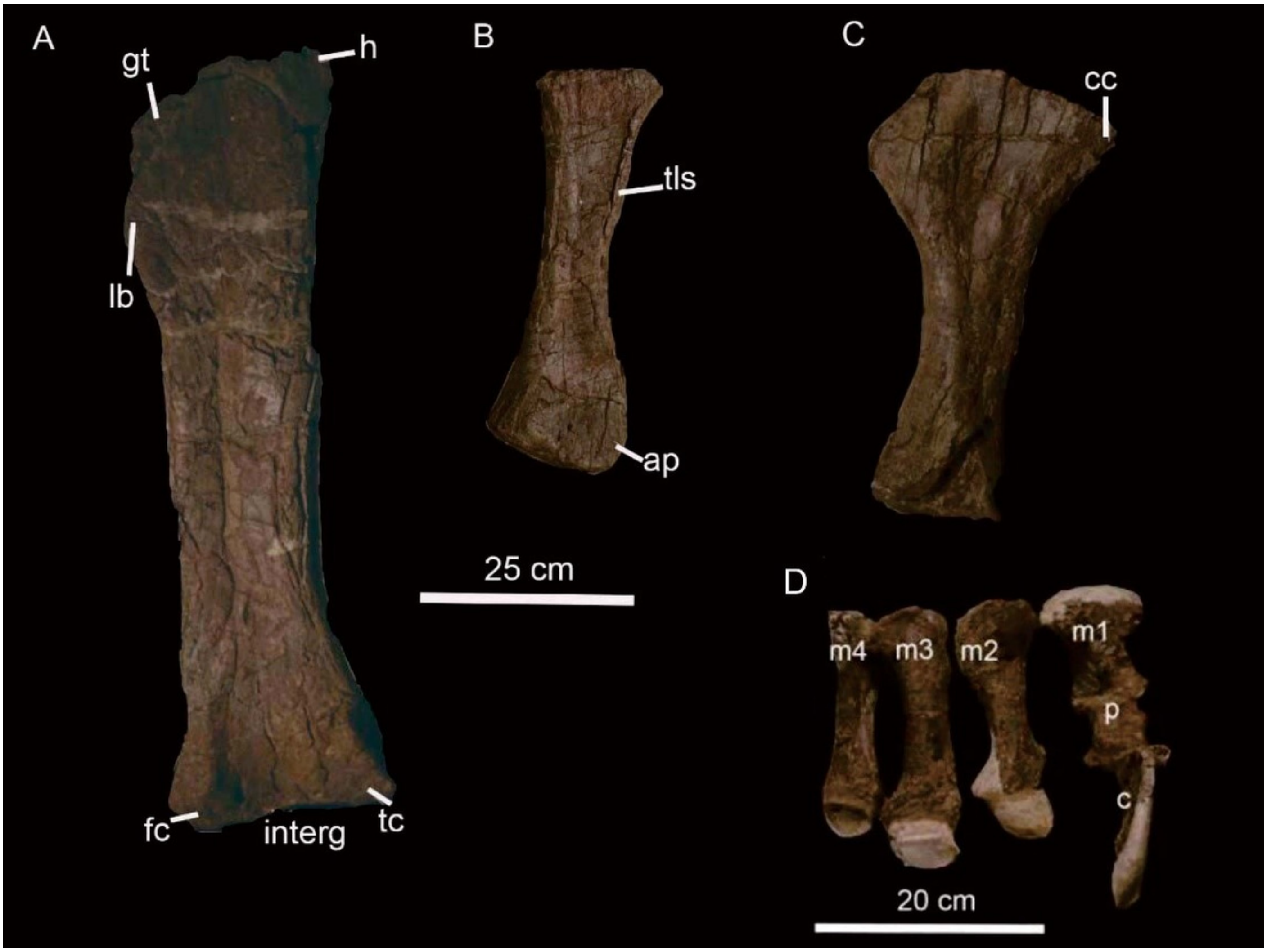

Figure 8

The reconstruction of the skull of *Liaoningotitan sinensis.* (The white part is the part missing from the holotype.)

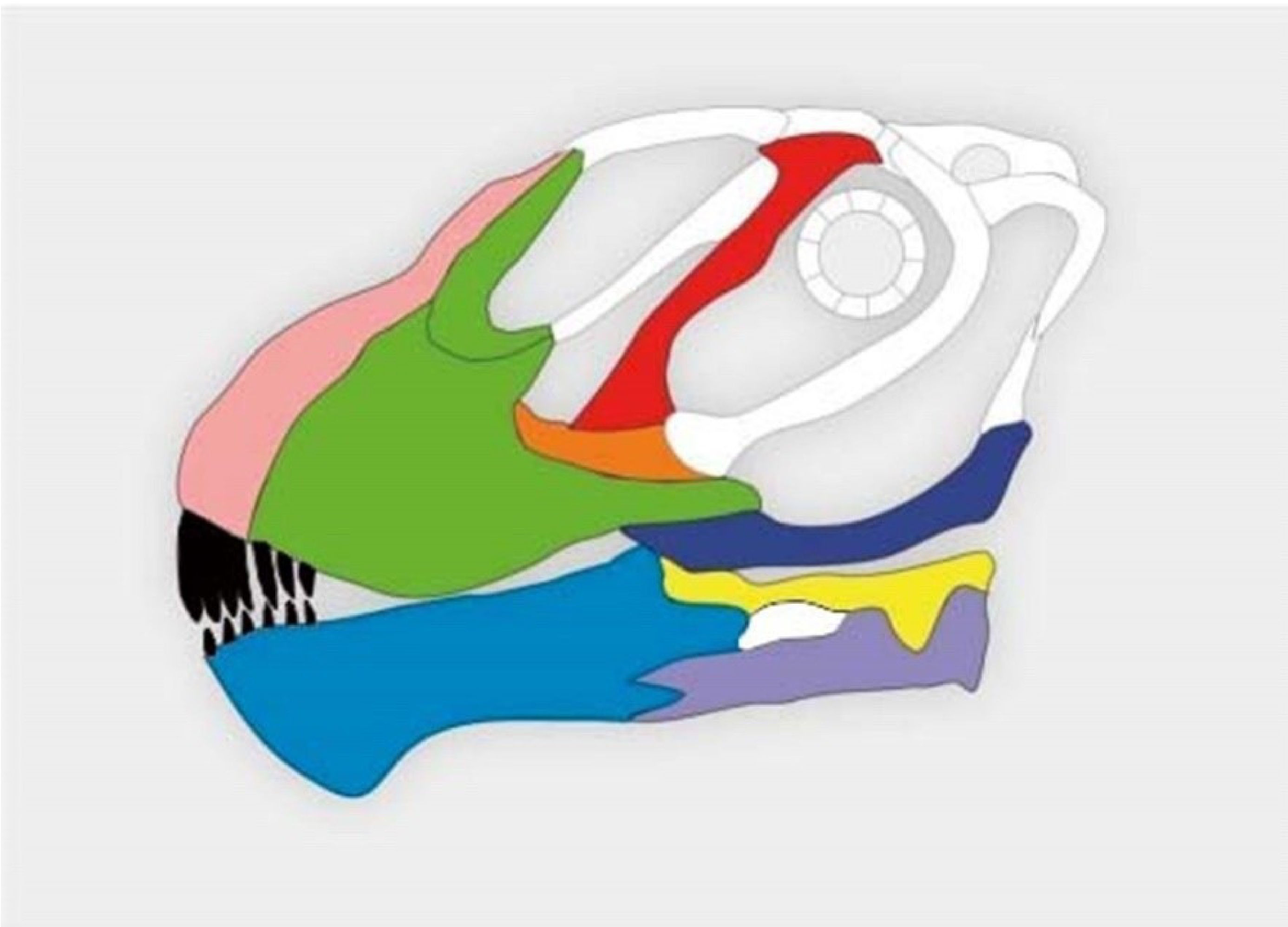

Figure 9

Phylogenetic analysis reduced consensus tree of *Liaoningotitan sinensis* PMOL-AD00112 (red)

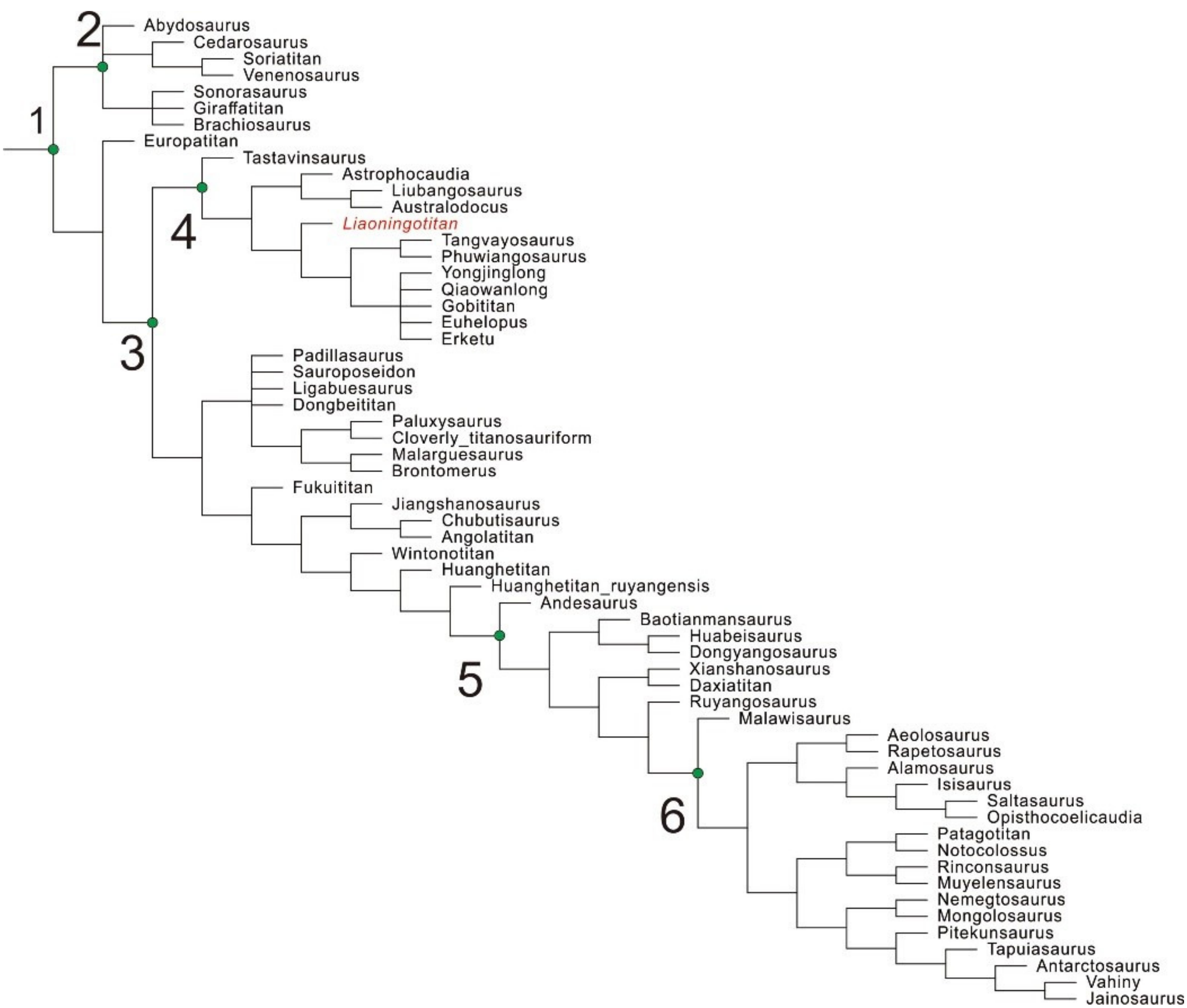

Figure 10

Skull height: skull length ratio in Eusauropoda. Linear regression (deep red line) and 95% confidence intervals (deep blue lines) show *Liaoningotitan* has a high skull height to length ratio, approaching that of *Omeisaurus tianfuensis*,[i] Mamen

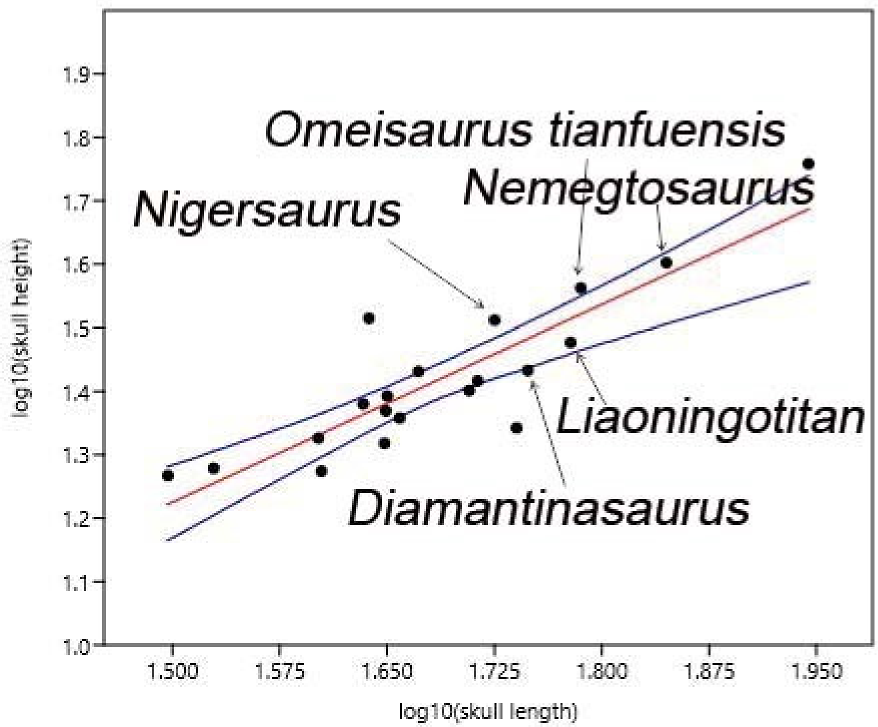

Figure 11

Ulna length: humerus length ratio in Eusauropoda. Linear regression (deep red line) and 95% confidence intervals (deep blue lines) show *Liaoningotitan* has a low ulna to humerus length ratio, close to that of *Omeisaurus maoianus*,[i] Mamenchisau

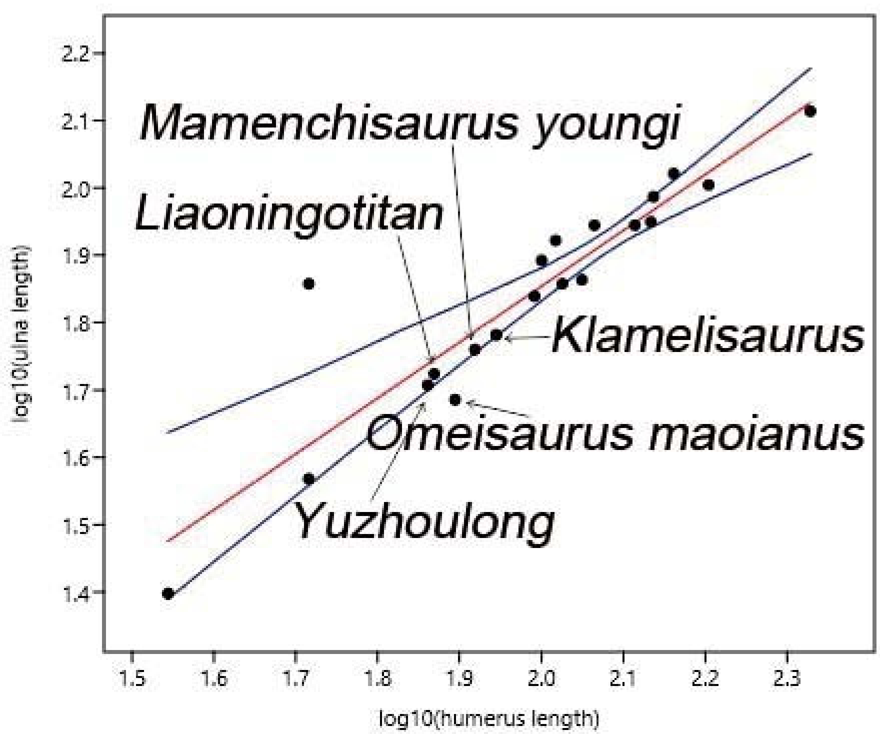

Figure 12

Tibia length: femur length ratio in Eusauropoda. Linear regression (deep red line) and 95% confidence intervals (deep blue lines) show *Liaoningotitan* has a low tibia length to femur length ratio, similar to distantly related *Shunosaurus lii*,[i